



Kent Academic Repository

Zare Oskouei, Morteza, Mohammadi-Ivatloo, Behnam, Abapour, Mehdi, Shafiee, Mahmood and Anvari-Moghaddam, Amjad (2020) *Privacy-Preserving Mechanism for Collaborative Operation of High-Renewable Power Systems and Industrial Energy Hubs*. *Applied Energy*, 283 . ISSN 0306-2619.

Downloaded from

<https://kar.kent.ac.uk/85752/> The University of Kent's Academic Repository KAR

The version of record is available from

<https://doi.org/10.1016/j.apenergy.2020.116338>

This document version

Author's Accepted Manuscript

DOI for this version

Licence for this version

CC BY-NC-ND (Attribution-NonCommercial-NoDerivatives)

Additional information

Versions of research works

Versions of Record

If this version is the version of record, it is the same as the published version available on the publisher's web site. Cite as the published version.

Author Accepted Manuscripts

If this document is identified as the Author Accepted Manuscript it is the version after peer review but before type setting, copy editing or publisher branding. Cite as Surname, Initial. (Year) 'Title of article'. To be published in *Title of Journal*, Volume and issue numbers [peer-reviewed accepted version]. Available at: DOI or URL (Accessed: date).

Enquiries

If you have questions about this document contact ResearchSupport@kent.ac.uk. Please include the URL of the record in KAR. If you believe that your, or a third party's rights have been compromised through this document please see our [Take Down policy](https://www.kent.ac.uk/guides/kar-the-kent-academic-repository#policies) (available from <https://www.kent.ac.uk/guides/kar-the-kent-academic-repository#policies>).

Privacy-preserving mechanism for collaborative operation of high-renewable power systems and industrial energy hubs

Morteza Zare Oskouei^a, Behnam Mohammadi-Ivatloo^b, Mehdi Abapour^a, Mahmood Shafiee^{c,*},
Amjad Anvari-Moghaddam^b

^aSmart Energy Systems Laboratory, Faculty of Electrical and Computer Engineering, University of Tabriz, Tabriz, Iran

^bDepartment of Energy Technology, Aalborg University, 9220 Aalborg East, Denmark

^cMechanical Engineering Group, School of Engineering, University of Kent, Canterbury CT2 7NT, UK

Abstract

Increased penetration of renewable energy sources (RESs) with non-uniformly distributed patterns as well as growing power consumption in industrialized countries have created an urgent need to use the backup energy supply units to boost the flexibility of bulk power systems. One of the prominent solutions is to deploy large-scale energy hubs in industrial parks to use the potentials of multi-carrier energy networks as additional reserves for power systems. However, centralized management of networked energy hubs may not be compatible with the power system operator when they are managed by private owners. Motivated by this observation, a privacy-preserving decision-making structure is proposed in this paper for collaborative operation of private industrial energy hubs (IEHs) and the renewable power system by considering high penetration of RESs, where the renewable power system operator (RPSO) interacts with industrial energy hubs operator (IEHO) in a leader-follower fashion. The proposed distributed structure is decomposed into a master problem and several sub-problems based on the Benders decomposition algorithm and solved in a decentralized manner to respect the private ownership of IEHs. A hybrid robust-stochastic approach is adopted to address the uncertainties of renewable power generation and the energy demands of local industrial consumers. Also, the impacts of the multi-energy demand response program (DRP) and energy storage systems on improving the performance of the integrated renewable energy system are investigated. The competency and robustness of the proposed collaborative decision-making structure and its benefits are examined through several case studies conducted on the IEEE 30-bus test system. Results show that if IEHs are successfully deployed in industrial parks, the total operation cost of the renewable power system decreases by up to 60%, renewable power curtailment reduces by 30%, and flexibility of the renewable power system enhances by increasing spinning reserve.

Keywords: Benders decomposition, demand response programs, energy storage systems, energy hub systems, privacy-preserving collaboration, renewable power curtailment.

*Corresponding author

Email address: m.shafiee@kent.ac.uk (Mahmood Shafiee)

1 Nomenclature

Acronyms

CHP	Combined heat and power.
DRP	Demand response program.
EES	Electrical energy storage.
IEHs	Industrial energy hubs.
IEHO	Industrial energy hubs operator.
PV	Photovoltaic.
P2H	Power-to-heat.
RPSO	Renewable power system operator.
RESs	Renewable energy sources.
WFs	Wind farms.

Indices (sets)

d (\mathcal{D})	Index of blocks of the piecewise linearization of the quadratic cost function.
g, e (\mathcal{G}, \mathcal{E})	Indices of thermal units and electrical energy storages.
h (\mathcal{H})	Index of industrial energy hubs.
i, j (\mathcal{I})	Indices of transmission buses.
k, q (\mathcal{K}, \mathcal{Q})	Indices of CHP units and P2H storages.
l, n (\mathcal{L}, \mathcal{N})	Indices of electrical and heat loads connected to industrial energy hubs.
m (\mathcal{M})	Index of electrical loads connected to renewable power system.
s (\mathcal{S})	Index of scenarios.
t (\mathcal{T})	Index of hourly intervals.
$w(\mathcal{W}), p$ (\mathcal{P})	Indices of WFs and PV parks.
ch, dch	Superscripts indicating charging and discharging status.

Parameters

a_g, b_g, c_g	Fuel consumption cost coefficients of thermal unit g .
COP_q	Coefficient of P2H storage performance.
$C_{g,in}^d, C_{g,fi}^d$	Initial and final amounts of generation cost in block d of the linearized cost function of thermal unit g .
IE, IH	Rate of incentive for electrical and heat demands variation.
$KN_{i,\Xi}, KN_{h,\Xi}$	Bus- Ξ and hub- Ξ incidence matrices.
$PD_{m,t}$	Forecasted electric demand at hour t .
$PD_{l,t,s}^{ini}, HD_{n,t,s}^{ini}$	Initial electrical and heat demands connected to industrial energy hubs.
RU_g, RD_g	Ramping up/down limits of thermal unit g .

t_b	Iteration numbers for Benders decomposition.
x_{ij}	Equivalent reactance of line ij .
XG_g^{on}, XG_g^{off}	Minimum on/off times of thermal unit g .
$P_{(\cdot),t}^f$	Forecasted renewable power output of WFs and PV parks at hour t .
$P_{g,in}^d, P_{g,fi}^d$	Initial and final amounts of power produced in block d of the linearized cost function of thermal unit g .
$\tilde{P}_{w,t}, \tilde{P}_{p,t}$	Maximum deviation of WF w and PV park p from forecasted values at hour t .
$\hat{P}_{tb,h,t,s}$	The amount of exchanged power, which is determined in the master problem.
SU_g, SD_g	Start-up/shut-down ramp limit of thermal unit g .
UT_g^0, DT_g^0	Duration of periods that thermal unit g has been online/offline prior to the first interval of the operating horizon.
Z_g^d	The slope of each block of the linearized cost function of thermal unit g .
ΔP_g^d	Length of each block of the linearized cost function of thermal unit g .
λ_g, HV	Natural gas price and natural gas heat value.
ρ_k, ρ_e, ρ_q	Maintenance cost of CHP unit, electrical storage, and P2H storage.
$\eta_{(\cdot)}$	Efficiency coefficient of various units.
α_l, α_n	Participation rate of electrical and heat demands in multi-energy DRP.
Γ_t	Uncertainty budget of renewable generation.
Π_{re}	Penalty prices for wind and solar power curtailments.
σ_s	Probability of each scenario.
$\underline{(\cdot)}, \overline{(\cdot)}$	Minimum/maximum bounds of variables.

Variables

$A_{(\cdot),t,s}$	Energy level of electrical and P2H storages at hour t in scenario s .
$C_{k,s}^{CHP}, C_{e,s}^{ES}, C_{q,s}^{P2H}$	The operation cost of CHP unit k , electrical storage e , and P2H storage q in scenario s .
$C_{l,n,s}^{MDR}$	Incentive compensation cost of multi-energy DRP in scenario s .
$C_{h,s}^{RPS}, C_h^{IEH}$	The total operation cost of renewable power system and industrial energy hub h .
$\hat{F}_{tb,h,t,s}^{IEH}$	Minimized sum of slack variables for industrial energy hub h at iteration t_b .
$H_{(\cdot),t,s}$	Heat production by IEHs' facilities at hour t in scenario s .
$H_{q,t,s}^{dir}$	Heat production by P2H storage q in direct mode of action at hour t in scenario s .
$\hat{O}_{tb,h}^{IEH}, \hat{O}_{tb}^{Total}$	The optimal operation cost of industrial energy hub h and total operational cost at iteration t_b .
$P_{(\cdot),t,s}$	Power output of various generation units at hour t in scenario s .

$p_{g,t,s}^d$	The power produced in block d of the piecewise linear cost function of thermal unit g at hour t in scenario s .
$P_{g,t}^{lo}, P_{g,t}^{up}$	Minimum/maximum available power output of thermal unit g at hour t .
$PC_{w,t,s}, PC_{p,t,s}$	Wind and solar power curtailments of WF w and PV park p at hour t in scenario s .
$PF_{ij,t,s}$	Power flow on line ij at hour t in scenario s .
$PD_{l,t,s}^{dr}, HD_{n,t,s}^{dr}$	Final electrical and heat demands profile at hour t in scenario s .
$SUC_{g,t}, SDC_{g,t}$	Start-up/shut-down costs of thermal unit g at hour t .
$\Delta P_{l,t,s}^{up}, \Delta P_{l,t,s}^{dw}$	Electrical demands change after multi-energy DRP implementation at hour t in scenario s .
$\Delta H_{n,t,s}^{up}, \Delta H_{n,t,s}^{dw}$	Heat demands change after multi-energy DRP implementation at hour t in scenario s .
$\delta_{i,t,s}$	Voltage phase angle at bus i at hour t in scenario s .
$u_{(\cdot),t,s}$	Binary variable to indicate status of facilities.
$y_{g,t}, \gamma_{g,t}$	Binary variable to indicate the status of thermal unit g at hour t .
$\tau_{t_b,h,t,s}^P, \Lambda_{t_b,h,t,s}^P$	Dual variables to create the optimality cutting plane and feasibility cutting plane.
$\xi_{h,t,s}^{P1}, \xi_{h,t,s}^{P2}$	Slack variables for the feasibility check.
$\beta_{w,t,s}, \beta_{p,t,s}$	Degree of the output power uncertainty of WF w and PV park p at hour t .
$r_{x,t,s}, \varepsilon_{t,s}$	Auxiliary variables in robust optimization model.
 <i>Functions</i>	
$F_g(P_{g,t,s})$	Fuel cost function of thermal unit g at hour t in scenario s .

2 1. Introduction

3 1.1. Motivation and significance

4 Nowadays, due to lack of proper facilities, such as lines' capacity, as well as ever-escalating power
5 consumption, restructured power systems face fundamental challenges to guarantee the stable operation
6 of the entire power system and satisfy technical constraints [1]. At the generation side, the penetration
7 of intermittent renewable energy sources (RESs) in power systems has dramatically increased, owing
8 to concerns about rising energy prices [2], environmental problems [3], and reliability requirements [3].
9 Although the utilization of high-power RESs, such as wind farms (WFs) and photovoltaic (PV) parks
10 has been proven to be an effective solution to address the existing concerns, the inherent variability
11 and non-uniform distribution of these sources have posed remarkable challenges for the safe operation
12 of renewable-based power systems [4]. According to some strong evidence, due to the aging of power
13 systems infrastructure, renewable power system operators (RPSOs) are obligated to curtail a significant
14 percentage of produced renewable power, especially at high penetration levels, to maintain the stability
15 and reliability of power systems [4, 5].

16 On the other hand, running on-site generation in large subscribers sites (e.g., industrial parks) has
17 received considerable attention in recent years. For example, on-site energy production in the industrial
18 sector of the U.S. in 2012 accounted for about 4% of the total power produced in the same year [6].
19 Accordingly, industrial parks have become one of the most influential players in the electrical industry
20 with the significant development they have had in recent years. The strategic role of industrial parks
21 in advancing power systems plans was extensively evaluated in recent studies from the perspective of
22 industrial consumers [7] and RPSO [8]. Most of these studies have emphasized the use of backup power
23 sources like electrical energy storage (EES) or energy conversion facilities to continuously supply industrial
24 demands [9]. Therefore, it is obvious that the traditional power systems and the installed protection
25 equipment are not suitable for compensating the excessive generation/load, yet upgrading the existing
26 power systems for short periods of operation is not economical.

27 Thanks to the recent advances in the modernization of interconnected energy systems, energy hub
28 systems have emerged as a promising platform in the form of multi-vector energy systems to overcome the
29 technical challenges as well as mitigate the potential risks associated with various players in power systems
30 [10]. The energy hub systems are composed of multiple input/output ports that create a stable interface
31 between different energy networks with regards to the advanced energy conversion facilities and energy
32 storage systems. These systems can provide unique economic and technical benefits for energy market
33 players and energy network operators and planners [11]. From the power system operators' point of view,
34 energy hub systems can boost the flexibility and reliability of power systems, enhance the resiliency of
35 the system, reduce operation cost, and decrease energy-wasting [12]. In addition, from the perspective of
36 energy system planners, the establishment of energy hubs in industrial parks, as a major energy consumer
37 [13], can help to realize the theory of localization of sustainable energy production and consumption [14].
38 Implementing this mechanism not only increases the flexibility of the interconnected energy systems, but
39 also enables industrial consumers to actively participate in wholesale energy markets and take advantage of
40 existing opportunities in different layers of energy networks [15]. On this basis, the industrial energy hubs
41 (IEHs) could be networked to form a multi-vector community at the sub-transmission and transmission
42 levels. In these circumstances, each IEH is managed by a private owner, which aims to supply local
43 demands using the existing facilities in energy hubs or via bilateral energy exchange with wholesale
44 energy markets at the lowest operating cost. The private IEHs are recognized as independent entities,
45 and these entities should cooperate with the power system in a privacy-preserving way [16]. Moreover, the
46 technical constraints must not be sacrificed to the existed distributed mechanisms. Accordingly, ensuring
47 the optimal collaborative operation of multiple private IEHs and power systems without compromising
48 privacy provisions is a challenging problem, especially when the various uncertainties are considered in
49 the scheduling process [17]. Therefore, it is necessary to draw up a holistic decentralized decision-making
50 structure for the coordinated operation of private IEHs and power systems to determine the optimal
51 energy dispatch among various players in the wholesale energy markets. By doing so, the power system
52 operator and industrial energy hubs operator (IEHO) can separately pursue their own goals within the
53 framework of the restructured energy systems.

54 In the following, various studies on the optimal operation of networked energy hubs are briefly reviewed

55 and then the technical contributions of this paper are presented.

56 *1.2. Related literature*

57 Due to the scope of this paper, there exists a large body of related studies that were focused on optimal
58 operation of networked energy hubs in power systems by incorporating RESs. In general, the related lit-
59 erature is categorized according to whether optimization programs were provided based on a traditionally
60 centralized dispatch approach or a decentralized framework. In terms of the centralized energy dispatch
61 of networked energy hubs, authors of [18] presented a centralized optimal energy management strategy
62 for the coordinated operation of grid-connected energy hubs in day-ahead electricity market. In the same
63 work, the decision-making about the integrated operation of the power system and energy hubs was made
64 by a common master controller in a centralized manner. A robust operation strategy for networked en-
65 ergy hubs was presented in [19] considering the uncertainty of renewable power production and demand
66 response programs (DRP). The main aim of that work was to reduce the total operation cost of multiple
67 energy hubs during the scheduling interval. In [20], a cost-effective centralized program was developed for
68 microgrids embedded with energy hubs with regards to the stochastic programming method and DRPs.
69 In a different approach, a multi-objective optimization program was developed in [21] with the aims of
70 minimizing the total operation cost of multiple energy hubs as well as reducing greenhouse gas emissions.
71 In this work, the produced power by RESs was considered as an uncertain parameter and was modeled
72 by a scenario-based method. A multi-step linearization method for the interconnected energy hubs was
73 examined in [22], which minimized the total operational cost of the networked energy hubs during the
74 scheduling period. Moreover, in [23], a two-level optimization problem was proposed for determining
75 optimal bidding/offering strategy of multiple networked energy hubs in the day-ahead electricity market
76 considering different sources of uncertainty. The problem was developed in the form of the centralized
77 dispatch approach, which was managed by the power system operator.

78 In addition to the utilized centralized decision-making schemes, there have been considerable efforts
79 in the research community to integrate energy hubs into power systems in decentralized and privacy-
80 preserving manners. In these kinds of studies, various distributed methods such as alternating direction
81 method of multipliers (ADMM) and decomposition methods were established to define decentralized
82 optimization problems for sustainable exploitation of networked energy hubs. For example, in [24], a
83 distributed energy management framework was derived from ADMM method to determine the optimal
84 scheduling of networked energy hubs. Authors of [25] proposed an auction-based regulation service mech-
85 anism for economic dispatch of the large-scale energy hubs in the context of the wholesale electricity
86 market. The proposed mechanism was solved in a decentralized manner using ADMM technique. In [26],
87 a distributed robust optimization method was proposed for making private coordination between energy
88 hubs and the power system considering the market price uncertainty. In that work, robust optimization
89 was considered to realize the worst-case of uncertain parameters in multi-carrier energy systems. In [27],
90 the leader-follower theory was applied in the framework of Benders decomposition for the optimal dispatch
91 of networked energy hubs. This theory can establish privacy-preserving collaborations among individual
92 energy hub operators and the power system operator. Finally, in [28, 29], distributed energy management

93 methods based on the decomposition algorithm were proposed for the robust optimal energy dispatch of
94 grid-connected energy hubs considering the uncertainty of renewable power generation.

95 By examining the above-mentioned studies, it can be seen that the principal focus of the technical
96 literature was on the optimal exploitation of multiple networked energy hubs aimed at reducing the total
97 operation cost of the multi-carrier energy systems. Nevertheless, ignoring the challenges posed by the high
98 penetration of RESs is the major gap in the aforementioned studies. It is worthwhile to mention that,
99 to the best of our knowledge no prior study in this field investigated the effects of new energy conversion
100 facilities, such as power-to-heat (P2H) storage, on improving the performance of the integrated renewable
101 energy systems in the presence of flexible demands and high-power and large-scale RESs. In addition,
102 very few studies in the literature have addressed the unique benefits of multi-energy DRP in advancing
103 the desired objectives of the energy system operators. Overall, we argue that the previous literature lacks
104 detailed models to address the various flexibility options, so further studies are needed to design a holistic
105 decision-making framework with respect to all available flexibility options.

106 *1.3. Technical contributions and paper structure*

107 This work aims to fill the knowledge gaps mentioned in the previous sub-section by applying a purely
108 mathematical-technical perspective. To this end, a privacy-preserving structure is presented for optimizing
109 RPSO/IEHO collaborations in an iterative manner by considering high penetration of WFs and PV parks.
110 The main objectives of the distributed optimization problem are to minimize the total operation cost of
111 the renewable power system and IEHs, reduce renewable power curtailment, and enhance the flexibility of
112 the integrated renewable energy system via realizing optimal coordination between different players. To
113 clarify the main contributions of this paper, the features of the proposed model are compared with other
114 published papers in Table 1. Eventually, the technical contributions of this study are as follow:

- 115 (1) A scalable and efficient structure with low complexity is proposed to determine the optimal day-
116 ahead operation of the renewable power system in coordination with private IEHs within the privacy-
117 preserving decision-making framework. In this regard, a decentralized two-stage robust-stochastic
118 security-constrained unit commitment (SCUC) model is developed for the collaborative operation
119 of networked IEHs and the renewable power system to facilitate the coordinated operation of RPSO
120 and IEHO as well as to preserve the operational privacy of these parties.
- 121 (2) A generalized Benders decomposition algorithm is employed to solve the proposed distributed robust-
122 stochastic model, which is in line with the prevalent leader-follower (RPSO-IEHO) relationships in
123 the energy management of the integrated renewable energy system. In the formed decomposition-
124 based program, both RPSO and IEHO seek common goals with respect to privacy provisions.
- 125 (3) A hybrid robust-stochastic strategy is implemented to handle the enforced operational uncertainties
126 associated with the renewable power output of WFs and PV parks and the energy demands of local
127 industrial consumers, and also to create less conservative and more trustworthy approaches. In
128 this regard, the robust optimization technique is employed to model uncertainties associated with

Table 1: Comparison of the contributions of related literature with the proposed structure.

References	Operation mode	Privacy	Coordinator	Resources	P2H storage	DRPs	Uncertainty modeling
[18]	Centralized	Sharing all data	Central supervisor	ECF + EES	×	×	Deterministic
[19]	Centralized	Sharing all data	Central supervisor	ECF + EES + RESs	×	✓	Robust
[20]	Centralized	Sharing all data	Central supervisor	ECF + RESs	×	✓	Stochastic
[21]	Centralized	Sharing local data	Central supervisor	ECF + EES + RESs	×	×	Stochastic
[22]	Centralized	Sharing all data	Central supervisor	ECF + EES	×	×	Deterministic
[23]	Centralized	Sharing all data	Central supervisor	ECF + EES + RESs	×	✓	Stochastic
[24]	Decentralized	Sharing power trading amount	PSO	ECF + EES + RESs	×	×	Deterministic
[25]	Decentralized	Sharing power trading amount	PSO	ECF	×	×	Deterministic
[26]	Decentralized	Sharing power trading amount	PSO	ECF + EES + RESs	×	×	Robust
[27]	Decentralized	Sharing power trading amount	ESO	ECF + EES	×	×	Deterministic
[28]	Decentralized	Sharing power trading amount	ESO	ECF + EES + RESs	×	×	Robust
[29]	Decentralized	Sharing power trading amount	ESO	ECF + EES + RESs	×	×	Robust
Proposed model	Decentralized	Sharing power trading amount	RPSO	ECF + EES + RESs	✓	✓	Hybrid robust-stochastic

*Note: ECF-Energy conversion facilities; PSO-Power system operator; ESO-Energy system operator

WFs and PV parks output powers, and the two-stage stochastic approach is used to handle the uncertainties caused by the energy demands of local industrial consumers.

- (4) In addition to the above points, the proposed joint optimization structure is extended based on the multi-energy DRP, EES, and P2H storage to minimize the total operation cost, immunize the power system in confronting the challenges of high-power RESs, as well as enhance operational flexibilities of the renewable power system by increasing spinning reserve.

The structure of this paper is organized as follows. Section 2 explains the proposed structure and presents the two-stage stochastic mathematical model for the optimal operation of the renewable power system in coordination with IEHs. The robust optimization method for handling the uncertainty of renewable power generation is presented in Section 3. In Section 4, the decentralized approach for the collaborative operation of multiple networked IEHs and renewable power system is explained. The numerical simulation and results for evaluating the proposed structure are provided in Section 5. Finally, conclusions and future works are drawn in Section 6.

2. Formulation of the proposed structure

In this section, the proposed distributed optimization model is formulated to ensure the optimal collaborative operations of networked IEHs with the renewable power system in the presence of various flexibility tools. The proposed model is composed of two independent entities, which are operated by separate decision-makers. The first entity has to do with RPSO as well as the private owners of IEHs are

147 considered as the second independent entity. The graphical description of the proposed structure is shown
 148 in Fig. 1. As can be seen, an integrated renewable energy system comprises a set \mathcal{H} of $H = |\mathcal{H}|$ IEHs,
 149 power transmission system interfaces, WF, PV park, and local industrial consumers. In the proposed
 150 structure, IEHs and local industrial consumers are managed by IEHO, and the rest of the system (i.e.,
 151 WF and PV park) are managed by RPSO. Each IEH is equipped with combined heat and power (CHP)
 152 units, EES, and P2H storage. An IEH has two input ports (electricity and gas connectors) and two output
 153 ports (electricity and heat connectors). The input ports are related to the purchased energies from the
 154 renewable power system and natural gas network, and output ports are used for trading electricity and
 155 thermal energy with industrial consumers, the district heating network, and the renewable power system.
 156 In other words, IEHO interacts with RPSO via bi-directional communications for creating an economic
 157 and secure operation using the constrained transmission system. On the contrary, IEHO has one-way
 158 collaboration with natural gas (at input ports) and district heating (at output ports) networks. In the
 159 developed decentralized structure, the privacy of operation data is preserved since the RPSO will not
 160 need all operation data of IEHs. To preserve the private ownership of IEHO, the conflicts of exchanging
 161 electrical power between RPSO and IEHO are resolved by the Benders decomposition algorithm in an
 162 iterative procedure. In this regard, the integrated two-stage robust-stochastic optimization model is
 163 decomposed into a master problem and a sub-problem considering the uncertainties of wind and PV
 164 generation as well as electricity and heat demands in the industrial customers' side. The master problem
 165 is handled by RPSO to determine day-ahead robust SCUC, and the sub-problem is solved independently
 166 by IEHO for optimizing the operation of IEHs by relying on the two-stage stochastic programming. The
 167 details of the day-ahead robust-stochastic SCUC formulation for each decision-maker are described in the
 168 following sub-sections. At first, the two-stage stochastic SCUC problem is developed for the proposed
 169 privacy-preserving model, which will be updated in Section 3 to implement the hybrid robust-stochastic
 170 concept.

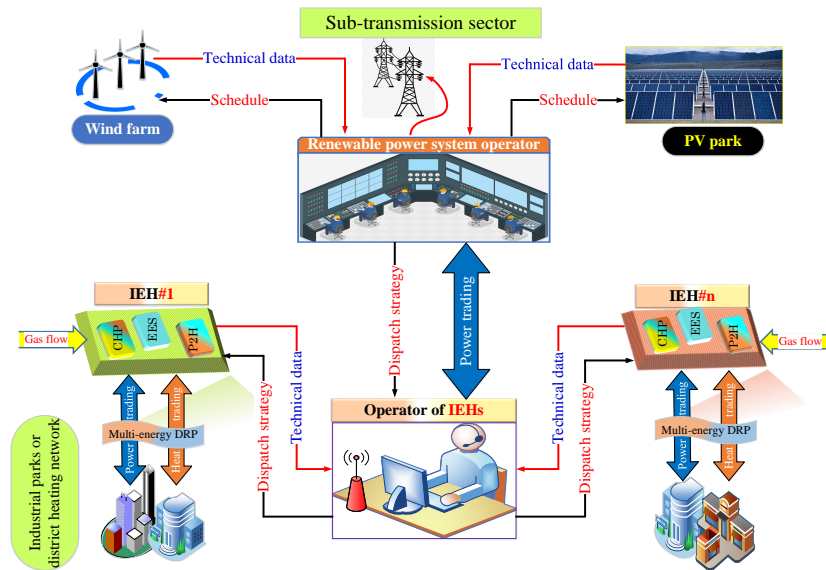


Fig. 1: Structure of decentral operation for multiple networked IEHs.

171 2.1. Decision-making of RPSO

172 The objective of RPSO's decision-making process is to minimize the total operation cost of supplying
 173 electrical loads outside of IEHs' services territories by thermal units and curtailing renewable power in
 174 optimal coordination with IEHO over the entire day-ahead scheduling horizon. The objective function
 175 formed to model this process, which is given in (1), contains two stages. The first stage includes the costs
 176 of start-up and shut-down of thermal units. This stage is independent of the stochastic process, therefore
 177 the start-up and shut-down costs are applied to all scenarios. The second stage of the objective function
 178 corresponds to the operation cost of thermal units and renewable power curtailment costs for WFs and
 179 PV parks. The second stage decision variables in the proposed two-stage stochastic programming model
 180 depend on the fluctuations in electricity and heat demands in the industrial customers' side, which are
 181 defined by different scenarios.

Min :

$$C^{RPS} = \sum_{t \in \mathcal{T}} \left[\sum_{g \in \mathcal{G}} (SUC_{g,t} + SDC_{g,t}) + \sum_{s \in \mathcal{S}} \sigma_s \cdot \left(\sum_{g \in \mathcal{G}} F_g(P_{g,t,s}) + \Pi_{re} \left(\sum_{w \in \mathcal{W}} PC_{w,t,s} + \sum_{p \in \mathcal{P}} PC_{p,t,s} \right) \right) \right] \quad (1)$$

182 2.1.1. Thermal units modeling

183 In this paper, the quadratic fuel cost function of thermal units is accurately approximated by a
 184 set of piecewise blocks to avoid complicating the optimization problem. The linearization process of the
 185 quadratic cost function using the least-squares criterion is illustrated in Fig. 2. The analytic representation
 186 of the linearization process is presented in (2)-(10) [30]. According to these equations, the fuel cost of
 187 thermal units can be defined by (10).

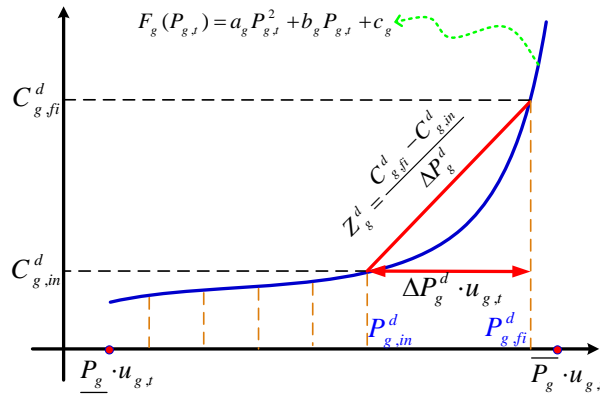


Fig. 2: Piecewise linear approximation of thermal units' quadratic cost function.

$$0 \leq p_{g,t,s}^d \leq \Delta P_g^d \cdot u_{g,t} \quad , \quad \forall g, t, s, d, \quad (2)$$

188

$$\Delta P_g^d = \frac{\overline{P}_g - P_g}{\mathcal{D}} \quad , \quad \forall g, d, \quad (3)$$

189

$$P_{g,in}^d = (d - 1) \cdot \Delta P_g^d + \underline{P}_g \quad , \quad \forall g, d, \quad (4)$$

$$P_{g,fi}^d = P_{g,in}^d + \Delta P_g^d, \quad \forall g, d, \quad (5)$$

$$P_{g,t,s} = \underline{P}_g \cdot u_{g,t} + \sum_{d \in \mathcal{D}} P_{g,t,s}^d, \quad \forall g, t, s, \quad (6)$$

$$C_{g,in}^d = a_g \cdot (P_{g,in}^d)^2 + b_g \cdot P_{g,in}^d + c_g, \quad \forall g, d, \quad (7)$$

$$C_{g,fi}^d = a_g \cdot (P_{g,fi}^d)^2 + b_g \cdot P_{g,fi}^d + c_g, \quad \forall g, d, \quad (8)$$

$$Z_g^d = \frac{C_{g,fi}^d - C_{g,in}^d}{\Delta P_g^d}, \quad \forall g, d, \quad (9)$$

$$F_g(P_{g,t,s}) = a_g \cdot \underline{P}_g^2 + b_g \cdot \underline{P}_g + c_g \cdot u_{g,t} + \sum_{d \in \mathcal{D}} (Z_g^d \cdot p_{g,t,s}^d), \quad \forall g, t, s. \quad (10)$$

The technical constraints of thermal units are presented by (11)-(26) [31]. The thermal units ramp-rates constraints for continuous intervals are indicated by (11)-(18). The power produced by each thermal unit is limited by upper and lower bounds as expressed by (11). The upper bound of the accessible power output of thermal units is constrained by shut-down ramp rate, i.e., (12), as well as by ramp-up and start-up ramp rates, i.e., (13). In addition, the lower bound of the accessible power output of thermal units is enforced by (15) and (16). Constraints (17) and (18) specify the on/off states of all units.

$$P_{g,t}^{lo} \leq P_{g,t,s} \leq P_{g,t}^{up}, \quad \forall g, t, s, \quad (11)$$

$$P_{g,t}^{up} \leq \bar{P}_g \cdot (u_{g,t} - \gamma_{g,t+1}) + SD_g \cdot \gamma_{g,t+1}, \quad \forall g, t, \quad (12)$$

$$P_{g,t}^{up} \leq P_{g,t-1} + RU_g \cdot u_{g,t-1} + SU_g \cdot y_{g,t}, \quad \forall g, t, \quad (13)$$

$$P_{g,t}^{up} \geq 0, \quad \forall g, t, \quad (14)$$

$$P_{g,t}^{lo} \geq \underline{P}_g \cdot u_{g,t}, \quad \forall g, t, \quad (15)$$

$$P_{g,t-1} - P_{g,t} \leq RD_g \cdot u_{g,t} + SD_g \cdot \gamma_{g,t}, \quad \forall g, t, \quad (16)$$

$$y_{g,t} - \gamma_{g,t} = u_{g,t} - u_{g,t-1}, \quad \forall g, t, \quad (17)$$

$$y_{g,t} + \gamma_{g,t} \leq 1, \quad \forall g, t. \quad (18)$$

Inequities (19)-(26) express minimum up/down times limits of each thermal unit. Constraints (19)-(22) are applied to satisfy the minimum up time constraint in the initial, middle, and final periods of the scheduling horizon, respectively. Likewise, the minimum down time limits can be formulated as (23)-(26).

$$\sum_{t=1}^{\mu_g} (1 - u_{g,t}) = 0, \quad \forall g, \quad (19)$$

$$\mu_g = \min \left\{ \mathcal{T}, (XG_g^{on} - UT_g^0) \cdot u_{g,0} \right\}, \quad \forall g, \quad (20)$$

$$\sum_{t=\nu}^{\nu+XG_g^{on}-1} u_{g,t} \geq XG_g^{on} \cdot y_{g,\nu} \quad , \quad \forall g, \quad \nu = [\mu_g + 1, \dots, \mathcal{T} - XG_g^{on} + 1], \quad (21)$$

$$\sum_{t=\nu}^{\mathcal{T}} (u_{g,t} - y_{g,t}) \geq 0 \quad , \quad \forall g, \quad \nu = [\mathcal{T} - XG_g^{on} + 2, \dots, \mathcal{T}], \quad (22)$$

$$\sum_{t=1}^{\varsigma_g} u_{g,t} = 0 \quad , \quad \forall g, \quad (23)$$

$$\varsigma_g = \min \left\{ \mathcal{T}, (XG_g^{off} - DT_g^0) \cdot (1 - u_{g,0}) \right\} \quad , \quad \forall g, \quad (24)$$

$$\sum_{t=\nu}^{\nu+XG_g^{off}-1} (1 - u_{g,t}) \geq XG_g^{off} \cdot \gamma_{g,\nu} \quad , \quad \forall g, \quad \nu = [\varsigma_g + 1, \dots, \mathcal{T} - XG_g^{off} + 1], \quad (25)$$

$$\sum_{t=\nu}^{\mathcal{T}} (1 - u_{g,t} - \gamma_{g,t}) \geq 0 \quad , \quad \forall g, \quad \nu = [\mathcal{T} - XG_g^{off} + 2, \dots, \mathcal{T}]. \quad (26)$$

where μ_g and ς_g represent the numbers of initial periods that thermal unit g must be online and offline.

The start-up and shut-down costs are expressed as constant values as (27) and (28), respectively.

$$SUC_{g,t} \geq suc_g \cdot y_{g,t}, \quad SUC_{g,t} \geq 0 \quad , \quad \forall g, t, \quad (27)$$

$$SDC_{g,t} \geq sdc_g \cdot \gamma_{g,t}; \quad SDC_{g,t} \geq 0 \quad , \quad \forall g, t. \quad (28)$$

2.1.2. Renewable power system technical constraints

The technical and operational constraints (29)-(35) must be applied to the safe operation of the renewable power system [31]. Constraint (29) ensures the curtailment rate of each WF/PV park cannot exceed the forecast values. The linearized DC-power flow model is used to calculate the amount of power flows from bus i to bus j which is presented in (30). The power flow in each line and voltage angle of each bus is restricted by its minimum and maximum limits, which are expressed by (31) and (32). It should be noted that, the value of the voltage angle in the slack bus must be equal to zero. This critical constraint is expressed by (33). The electrical demands of the renewable power system should be met by the output power of the thermal units, WFs, and PV parks as well as the power exchanged with IEHs considering the power flow limits between the system buses. Hence, the power balance constraint at bus j can be described by (34). The amount of transferred power from the renewable power system to IEHs and vice versa should be limited by (35). Note that, $P_{h,t,s}$ is considered as a free variable. The positive amount shows the imported power from the renewable power system into the IEHs and the negative amount demonstrates the delivered power from IEHs into the renewable power system.

$$0 \leq PC_{x,t,s} \leq P_{x,t}^f \quad , \quad \forall x \in \{w, p\}, t, s. \quad (29)$$

$$PF_{ij,t,s} = \frac{\delta_{i,t,s} - \delta_{j,t,s}}{x_{ij}} \quad , \quad \forall i, j, t, s, \quad (30)$$

$$-PF_{ij} \leq PF_{ij,t,s} \leq PF_{ij} \quad , \quad \forall i, j, t, s, \quad (31)$$

239

$$-\pi \leq \delta_{i,t,s} \leq +\pi, \quad \forall i, t, s, \quad (32)$$

$$\delta_{slack,t,s} = 0, \quad \forall t, s, \quad (33)$$

$$\sum_{g \in \mathcal{G}} KN_{i,g} \cdot P_{g,t,s} + \sum_{w \in \mathcal{W}} KN_{i,w} \cdot (P_{w,t}^f - PC_{w,t,s}) + \sum_{p \in \mathcal{P}} KN_{i,p} \cdot (P_{p,t}^f - PC_{p,t,s}) - \quad (34)$$

$$\sum_{h \in \mathcal{H}} KN_{i,h} \cdot P_{h,t,s} - \sum_{m \in \mathcal{M}} KN_{i,m} \cdot PD_{m,t} = \sum_{j \in \mathcal{I}} KN_{i,j} \cdot PF_{ij,t,s}, \quad \forall i, t, s,$$

$$\underline{P}_h \leq P_{h,t,s} \leq \overline{P}_h, \quad \forall h, t, s. \quad (35)$$

2.2. Decision-making of individual IEHs

Each IEH ($\forall h$) possesses EES, CHP unit, and P2H storage as the energy conversion facilities, for supplying local electricity and heat demands in industrial parks while interacting with RPSO. In the proposed decentralized approach, the energy hub model can be easily developed to include other energy conversion facilities. In the decision-making process of each IEH, the aim is to minimize the total operation cost of each IEH over the entire day-ahead scheduling horizon considering the uncertainty of local industrial consumers' demands. The objective function of private IEHs is formulated in (36) and (37) as follows:

$$\text{Min} : \quad C^{IEHO} = \sum_{h \in \mathcal{H}} C_h^{IEH}, \quad (36)$$

$$C_h^{IEH} = \sum_{s \in \mathcal{S}} \sigma_s \left[\sum_{k \in \mathcal{K}} C_{k,s}^{CHP} + \sum_{q \in \mathcal{Q}} C_{q,s}^{P2H} + \sum_{e \in \mathcal{E}} C_{e,s}^{ES} + \sum_{\substack{(l,n) \in \\ (\mathcal{L}, \mathcal{N})}} C_{l,n,s}^{MDR} \right], \quad \forall h. \quad (37)$$

The first term of (37) (i.e., $C_{k,s}^{CHP}$) indicates the fuel and maintenance costs of CHP units, which can be calculated by (38) [32]. The second term (i.e., $C_{q,s}^{P2H}$) refers to the maintenance cost of P2H storages, which can be defined by (39). The EES degradation cost (i.e., $C_{e,s}^{ES}$) due to frequent charge and discharge is considered in the third term. The accumulated degradation cost of EESs in IEHs are characterized by (40) [27]. Eventually, the final term (i.e., $C_{l,n,s}^{MDR}$) of (37) represents the multi-energy DRP compensation cost, where the incentive compensation costs paid to the industrial customers to perform the multi-energy DRP can be defined as (41) [33]. These cost functions are determined by the optimal scheduling of private IEHs in the optimal coordinated operation with the renewable power system.

$$C_{k,s}^{CHP} = \sum_{t \in \mathcal{T}} \left(\frac{\lambda_g}{\eta_k \cdot HV} \cdot P_{k,t,s} \right) + (\rho_k \cdot P_{k,t,s}), \quad \forall k, s, \quad (38)$$

$$C_{q,s}^{P2H} = \sum_{t \in \mathcal{T}} \rho_q \cdot (H_{q,t,s}^{ch} + H_{q,t,s}^{dch}), \quad \forall q, s, \quad (39)$$

$$C_{e,s}^{ES} = \sum_{t \in \mathcal{T}} \rho_e \cdot (P_{e,t,s}^{ch} + P_{e,t,s}^{dch}), \quad \forall e, s, \quad (40)$$

$$C_{l,n,s}^{MDR} = \sum_{t \in \mathcal{T}} \left[\left(IE \times (\Delta P_{l,t,s}^{up} + \Delta P_{l,t,s}^{dw}) \right) + \left(IH \times (\Delta H_{n,t,s}^{up} + \Delta H_{n,t,s}^{dw}) \right) \right], \quad \forall l, n, s. \quad (41)$$

The operational constraints governing IEHs are described below.

263 *2.2.1. CHP units constraints*

264 The heat and electric power produced by CHP units have mutual dependence, which is determined
 265 by the special feasible operation region (FOR) for each unit. The feasible region model associated with
 266 the considered CHP units in this article is shown in Fig. 3. The operational boundary (ABCD) of CHP
 267 units can be formulated by linear constraints, as given in (42)-(44) [34]. In these constraints, M is a large
 268 number (e.g., 1000). Moreover, constraints (45) and (46) ensure that the power and heat production of
 269 CHP units are at the acceptable levels.

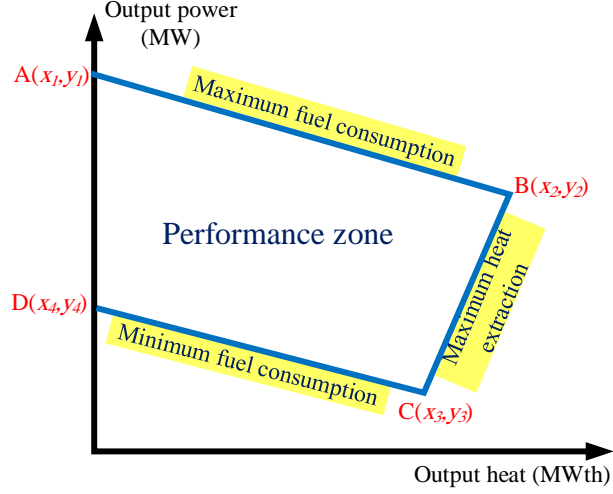


Fig. 3: FOR model for CHP units.

$$P_{k,t,s} - P_{k,A} - \frac{P_{k,A} - P_{k,B}}{H_{k,A} - H_{k,B}} \cdot (H_{k,t,s} - H_{k,A}) \leq 0, \quad \forall k, t, s, \quad (42)$$

270
$$P_{k,t,s} - P_{k,B} - \frac{P_{k,B} - P_{k,C}}{H_{k,B} - H_{k,C}} \cdot (H_{k,t,s} - H_{k,B}) \geq -(1 - u_{k,t,s}) \cdot M, \quad \forall k, t, s, \quad (43)$$

271
$$P_{k,t,s} - P_{k,C} - \frac{P_{k,C} - P_{k,D}}{H_{k,C} - H_{k,D}} \cdot (H_{k,t,s} - H_{k,C}) \geq -(1 - u_{k,t,s}) \cdot M, \quad \forall k, t, s, \quad (44)$$

272
$$\underline{P}_k \cdot u_{k,t,s} \leq P_{k,t,s} \leq \overline{P}_k \cdot u_{k,t,s}, \quad \forall k, t, s, \quad (45)$$

273
$$0 \leq H_{k,t,s} \leq \overline{H}_k \cdot u_{k,t,s}, \quad \forall k, t, s. \quad (46)$$

274 *2.2.2. P2H storages constraints*

275 The operational constraints related to P2H storages are defined as (47)-(54). The dynamic energy
 276 balance of the P2H storage in each hour is expressed by (47). The capacity limit of the P2H storage is
 277 given by (48). The initial ($t = 0$) and final ($t = \mathcal{T}$) state of charge of the P2H storage is limited to (49).
 278 The allowable ranges of charging and discharging thermal energy in this storage are limited by (50) and
 279 (51), respectively. The generated thermal energy by the P2H storage can be delivered to the industrial
 280 customers (or district heating networks) or stored in the reservoir, as stated in (52). Here, constraint (53)
 281 demonstrates the allowable limit for input power from the renewable power system into the P2H storage.

282 The inequality (54) ensures that each P2H storage cannot simultaneously charge and discharge.

$$A_{q,t,s} = (1 - \eta_q) \cdot A_{q,t-1,s} + H_{q,t,s}^{ch} - H_{q,t,s}^{dch} - \beta_{loss} \cdot SU_{q,t,s} + \beta_{gain} \cdot SD_{q,t,s} \quad , \quad \forall q, t, s, \quad (47)$$

$$283 \quad \underline{A}_q \leq A_{q,t,s} \leq \overline{A}_q \quad , \quad \forall q, t, s, \quad (48)$$

$$284 \quad A_{q,0,s} = A_{q,\mathcal{T},s} \quad , \quad \forall q, s, \quad (49)$$

$$285 \quad 0 \leq H_{q,t,s}^{ch} \leq \overline{H}_q^{ch} \cdot u_{q,t,s}^{ch} \quad , \quad \forall q, t, s, \quad (50)$$

$$286 \quad 0 \leq H_{q,t,s}^{dch} \leq \overline{H}_q^{dch} \cdot u_{q,t,s}^{dch} \quad , \quad \forall q, t, s, \quad (51)$$

$$287 \quad H_{q,t,s}^{ch} + H_{q,t,s}^{dir} = COP_q \cdot P_{q,t,s} \quad , \quad \forall q, t, s, \quad (52)$$

$$288 \quad 0 \leq P_{q,t,s} \leq \overline{P}_q \quad , \quad \forall q, t, s, \quad (53)$$

$$289 \quad u_{q,t,s}^{ch} + u_{q,t,s}^{dch} \leq 1 \quad , \quad \forall q, t, s. \quad (54)$$

290 where the binary variables (i.e., $u_{q,t,s}^{ch}$ and $u_{q,t,s}^{dch}$) represent the charging and discharging status of P2H
291 storages.

292 2.2.3. EES system constraints

293 The operation of each EES is defined by the following relationships. Based on (55), the electrical
294 energy level of each EES in a scheduling interval is calculated. The capacity level of each EES should be
295 restricted in its minimum and maximum limits, which is modeled by (56). According to (57), the state of
296 charge of each EES must be equal to $A_{e,0,s}$ at the end of the scheduling period. The charge and discharge
297 limitations of each EES are imposed by (58) and (59), respectively. Eventually, constraint (60) is used to
298 avoid charging/discharging of each EES at the same time.

$$A_{e,t,s} = A_{e,t-1,s} + \eta_e^{ch} \cdot P_{e,t,s}^{ch} - \frac{P_{e,t,s}^{dch}}{\eta_e^{dch}} \quad , \quad \forall e, t, s, \quad (55)$$

$$299 \quad \underline{A}_e \leq A_{e,t,s} \leq \overline{A}_e \quad , \quad \forall e, t, s, \quad (56)$$

$$300 \quad A_{e,0,s} = A_{e,\mathcal{T},s} \quad , \quad \forall e, s, \quad (57)$$

$$301 \quad \underline{P}_e^{ch} \cdot u_{e,t,s}^{ch} \leq P_{e,t,s}^{ch} \leq \overline{P}_e^{ch} \cdot u_{e,t,s}^{ch} \quad , \quad \forall e, t, s, \quad (58)$$

$$302 \quad \underline{P}_e^{dch} \cdot u_{e,t,s}^{dch} \leq P_{e,t,s}^{dch} \leq \overline{P}_e^{dch} \cdot u_{e,t,s}^{dch} \quad , \quad \forall e, t, s, \quad (59)$$

$$303 \quad u_{e,t,s}^{ch} + u_{e,t,s}^{dch} \leq 1 \quad , \quad \forall e, t, s. \quad (60)$$

304 where the binary variables (i.e., $u_{e,t,s}^{ch}$ and $u_{e,t,s}^{dch}$) model the charging and discharging status of EESs.

306 2.2.4. Multi-energy DRP constraints

307 DRP is one of the most flexible tools for the management of IEHs behavior to interact effectively
308 with the renewable power system by exploiting the economic opportunities available in the industrial
309 customers' side. In this paper, multi-energy DRP is performed to minimize the total operation cost of the
310 integrated renewable energy system, reduce renewable power curtailments, and enhance the flexibility of

311 the renewable power system by creating optimal coordination between RPSO and IEHO in an iterative
312 manner. DRPs are divided into two categories: the price-based DRP and the incentive-based DRP. In this
313 study, multi-energy DRP is considered based on the incentive-based manner, which is performed using
314 direct load control (DLC) program. Hence, the incentive compensation costs are paid to the participating
315 customers in the form of the DLC program. Based on (61) and (62), the DLC program is performed on
316 the electrical and heat demands with respect to the percentage of participation of each consumer in the
317 multi-energy DRP. After the implementation of multi-energy DRP, the final electrical and heat profiles
318 are determined using (63) and (64) [33].

$$\begin{cases} \Delta P_{l,t,s}^{up} \leq \alpha_l \times PD_{l,t,s}^{ini}, & \forall l, t, s, \\ \Delta P_{l,t,s}^{dw} \leq \alpha_l \times PD_{l,t,s}^{ini}, & \forall l, t, s, \end{cases} \quad (61)$$

$$\begin{cases} \Delta H_{n,t,s}^{up} \leq \alpha_n \times HD_{n,t,s}^{ini}, & \forall n, t, s, \\ \Delta H_{n,t,s}^{dw} \leq \alpha_n \times HD_{n,t,s}^{ini}, & \forall n, t, s, \end{cases} \quad (62)$$

$$PD_{l,t,s}^{dr} = \Delta P_{l,t,s}^{up} - \Delta P_{l,t,s}^{dw} + PD_{l,t,s}^{ini} \quad \forall l, t, s, \quad (63)$$

$$HD_{n,t,s}^{dr} = \Delta H_{n,t,s}^{up} - \Delta H_{n,t,s}^{dw} + HD_{n,t,s}^{ini} \quad \forall n, t, s. \quad (64)$$

319 2.2.5. IEHs' energy balancing

320 The IEHO manages the energy balance in each IEH by considering localized energy generation, energy
321 curtailments, as well as power imported/exported from/to the renewable power system. Constraints (65)
322 and (66) are used to make the energy balance between energy consumed by local demands (i.e., $PD_{l,t,s}^{ini}$
323 and $HD_{n,t,s}^{ini}$) and generated/traded energy in each IEH. It should be noted that the modified energy
324 demands after implementing multi-energy DRP are used rather than the initial energy demands in the
325 supply-demand constraints.

$$\begin{aligned} P_{h,t,s} + \sum_{e \in E} KN_{h,e} \cdot (P_{e,t,s}^{dch} - P_{e,t,s}^{ch}) + \sum_{k \in \mathcal{K}} KN_{h,k} \cdot P_{k,t,s} - \sum_{q \in \mathcal{Q}} KN_{h,q} \cdot P_{q,t,s} \\ - \sum_{l \in \mathcal{L}} KN_{h,l} \cdot PD_{l,t,s}^{dr} = 0, \quad \forall h, t, s, \end{aligned} \quad (65)$$

$$\begin{aligned} \sum_{k \in \mathcal{K}} KN_{h,k} \cdot H_{k,t,s} + \sum_{q \in \mathcal{Q}} KN_{h,q} \cdot (H_{q,t,s}^{dch} - H_{q,t,s}^{ch} + H_{q,t,s}^{dir}) - \\ \sum_{n \in \mathcal{N}} KN_{h,n} \cdot HD_{n,t,s}^{dr} = 0, \quad \forall h, t, s. \end{aligned} \quad (66)$$

326 3. Hybrid robust-stochastic model

327 In the above-described model, the uncertainty of renewable generation was neglected and the output
328 power of WFs and PV parks was perfectly forecasted. Since the uncertainty of RESs is more vital than

329 the energy demands, the RPSO prefers to apply a risk-based method to handle the uncertainty associated
330 with renewable powers, while the IEHO tries to manage the fluctuations of electrical and heat demands
331 of local industrial consumers using stochastic programming based on a Monte-Carlo (MC) simulation.
332 Compared to the stochastic programming, which requires the probability distribution function (PDF) or
333 fuzzy membership set of uncertain parameters, the robust approach describes uncertain parameters by
334 descriptive statistics. Therefore, in such models, complex calculations resulting from scenario counting
335 are avoided. In the proposed privacy-preserving decision-making structure, the mathematical definition
336 of the distributed robust-stochastic approach to realize the worst case is as follows.

337 After adopting the budget of uncertainty, the uncertainty set of WFs and PV parks is described by
338 (67)-(69) [35]. The degree of uncertainty of RESs in period t can be controlled by variable $\beta_{x,t,s}$. The
339 value of $\beta_{x,t,s} = 0$ demonstrates that there is no uncertainty in renewable power production in period t ,
340 while $\beta_{x,t,s} = 1$ demonstrates that the maximum renewable power uncertainty occurs in period t . The
341 robustness level of the solution can be controlled by the budget of uncertainty (i.e., Γ_t). The budget of
342 the uncertainty parameter can change from 0 to 1 in each scheduling interval. The greater value of Γ_t
343 (e.g., 1) means that RPSO has selected a highly conservative state in period t . In contrast, a lower value
344 of Γ_t means that the uncertain parameter is almost neglected in period t .

$$P_{x,t} \in \left[P_{x,t}^f - \beta_{x,t,s} \cdot \tilde{P}_{x,t}, P_{x,t}^f + \beta_{x,t,s} \cdot \tilde{P}_{x,t} \right], \quad \forall x \in \{w, p\}, t, s, \quad (67)$$

$$0 \leq \beta_{x,t,s} \leq 1, \quad \forall x \in \{w, p\}, t, s, \quad (68)$$

$$\sum_{w \in \mathcal{W}} \beta_{w,t,s} + \sum_{p \in \mathcal{P}} \beta_{p,t,s} \leq \Gamma_t \quad \forall t, s. \quad (69)$$

347 Based on the uncertainty model of the RESs presented in (67)-(69), the renewable power curtailment
348 constraint, which was shown in (29), and energy balance constraint, which was shown in (34), can be
349 converted to (70) and (71), respectively.

$$0 \leq PC_{x,t,s} \leq P_{x,t}^f + \beta_{x,t,s} \cdot \tilde{P}_{x,t}, \quad \forall x \in \{w, p\}, t, s, \quad (70)$$

$$\begin{aligned} \sum_{x \in \mathcal{X}} KN_{i,x} \cdot (P_{x,t}^f - \beta_{x,t,s} \cdot \tilde{P}_{x,t}) &\geq \sum_{x \in \mathcal{X}} KN_{i,x} \cdot PC_{x,t,s} + \sum_{m \in \mathcal{M}} KN_{i,m} \cdot PD_{m,t} + \\ \sum_{j \in \mathcal{I}} KN_{i,j} \cdot PF_{ij,t,s} - \sum_{g \in \mathcal{G}} KN_{i,g} \cdot P_{g,t,s} - \sum_{h \in \mathcal{H}} KN_{i,h} \cdot P_{h,t,s}, &\quad \forall x \in \{w, p\}, i, t, s. \end{aligned} \quad (71)$$

351 Subject to: (68) and (69)

352 According to the duality theory [36], constraint (71) can be converted to (72)-(74).

$$\begin{aligned} \sum_{x \in \mathcal{X}} KN_{i,x} \cdot (P_{x,t}^f - r_{x,t,s}) - (\varepsilon_{t,s} \cdot \Gamma_t) &= \sum_{x \in \mathcal{X}} KN_{i,x} \cdot PC_{x,t,s} + \sum_{m \in \mathcal{M}} KN_{i,m} \cdot PD_{m,t} + \\ \sum_{j \in \mathcal{I}} KN_{i,j} \cdot PF_{ij,t,s} + \sum_{h \in \mathcal{H}} KN_{i,h} \cdot P_{h,t,s} - \sum_{g \in \mathcal{G}} KN_{i,g} \cdot P_{g,t,s}, &\quad \forall x \in \{w, p\}, i, t, s, \end{aligned} \quad (72)$$

$$r_{x,t,s} + \varepsilon_{t,s} \geq \tilde{P}_{x,t}, \quad \forall x \in \{w, p\}, t, s, \quad (73)$$

$$r_{x,t,s}, \varepsilon_{t,s} \geq 0, \quad \forall x \in \{w, p\}, t, s. \quad (74)$$

where $r_{x,t,s}$ and $\varepsilon_{t,s}$ are the dual variables of the initial problem. The constraint (70) can also be transformed into (75) based on the duality theory.

$$0 \leq PC_{x,t,s} \leq P_{x,t}^f + r_{x,t,s} + \varepsilon_{t,s} \cdot \Gamma_t, \quad \forall x \in \{w, p\}, t, s. \quad (75)$$

After performing this mathematical process, the distributed robust-stochastic SCUC model can be formulated as mixed-integer linear programming (MILP) problem, which can be solved using commercial optimization packages. The summary of the proposed model is as follows.

- **Objective function of the leader:** RPSO aims to minimize the total operating cost by (1).
- Constraints of the leader problem:
 1. Applying thermal unit constraints based on (2)-(28).
 2. Applying renewable power curtailments constraints based on (75).
 3. Satisfying technical limitations based on (30)-(33), (35), and (72)-(74).
- **Objective function of the follower:** IEHO aims to minimize their own operating costs by (36)-(41).
- Constraints of the follower problems:
 1. Applying CHP units constraints based on (42)-(46).
 2. Applying P2H storages constraints based on (47)-(54).
 3. Applying EES systems constraints based on (55)-(60).
 4. Performing multi-energy DRP based on (61)-(64).
 5. Satisfying energy balance limitations based on (65) and (66).

4. Decentral solution methodology

The proposed distributed robust-stochastic SCUC problem is in an MILP format that guarantees the global optimal solution. However, the operating problem of the renewable power system and IEHs are interdependent through (72), which due to this constraint, it is not possible to solve the optimization problems separately. Based on (72), the RPSO and IEHO are coupled with the hourly scheduling and exchange of electrical power at IEHs' nodes. To address this issue, the standard Benders decomposition algorithm is applied to solve the proposed collaborative operation model in a decentralized manner while preserving the privacy of RPSO and IEHO. Benders decomposition algorithm is one of the most efficient decomposition techniques, which is used in power systems. The details of the implementation of the Benders decomposition algorithm are given in [37].

The Benders decomposition can be utilized to exploit a separable framework for the two-stage robust-stochastic SCUC problem, where this problem is decomposed into an optimization problem as a master

384 problem for RPSO and several optimal operation problems at the level of IEHO as sub-problems, which
 385 will be solved separately.

386 (I) **Master problem (MP)**: RPSO is responsible for ensuring the operational security of the renewable
 387 power system and tries to minimize the total operation cost, including operation cost of thermal units
 388 and compensation cost of renewable power curtailments according to the optimal trade policy of power
 389 with IEHs. The general structure of the master problem at iteration t_b is formulated as (76).

$$\begin{aligned}
 \text{Min :} \quad & \hat{O}_{t_b}^{Total}, \\
 \hat{O}_{t_b}^{Total} = & C^{RPS} + \sum_{h \in \mathcal{H}} O_h^{app}, \\
 \text{s.t.} \quad & \text{Operational constraints of the leader problem,} \\
 & \text{Feasibility cutting plane,} \\
 & \text{Optimality cutting plane.}
 \end{aligned} \tag{76}$$

390 where O_h^{app} is a non-negative continuous variable that represents the operation cost of the IEH h as
 391 approximated by the RPSO. At each iteration, RPSO minimizes the total operation cost (i.e., $\hat{O}_{t_b}^{Total}$) as
 392 an effective lower bound (LB) of the optimal robust-stochastic SCUC model by considering all available
 393 Benders cuts constraints ($LB = \hat{O}_{t_b}^{Total}$).

394 (II) **Sub-problem of the h th IEH**: After solving the master problem at each iteration, the optimal
 395 power trade schedule in the form of a tentative solution is passed to sub-problems that can be handled
 396 in parallel by individual IEHs. The IEHO determines the optimal dispatch of each IEH in two phases.
 397 In the first phase, IEHO checks whether the power exchange schedule obtained from the master problem
 398 is practically feasible by considering operational and technical constraints in each IEH operation. The
 399 feasibility check sub-problem for the h th IEH at iteration t_b is stated as:

$$\begin{aligned}
 \text{Min :} \quad & \hat{F}_{t_b, h, t, s}^{IEH} = \xi_{h, t, s}^{P1} + \xi_{h, t, s}^{P2}, \\
 \text{s.t.} \quad & \text{Operational constraints of followers problems,} \\
 & P_{h, t, s} + \xi_{h, t, s}^{P1} = \hat{P}_{t_b, h, t, s} + \xi_{h, t, s}^{P2}; \quad (\Lambda_{t_b, h, t, s}^P), \\
 & \xi_{h, t, s}^{P1}, \xi_{h, t, s}^{P2} \geq 0.
 \end{aligned} \tag{77}$$

400 where $\hat{P}_{t_b, h, t, s}$ is related to the power exchange amounts, which is obtained from the master problem.
 401 Moreover, $\xi_{h, t, s}^{P1}$ and $\xi_{h, t, s}^{P2}$ are non-negative slack variables, and $\Lambda_{t_b, h, t, s}^P$ is the dual variable associated
 402 with the first constraint of the problem (77). For a non-zero optimal objective value ($\hat{F}_{t_b, h, t, s}^{IEH} \neq 0$),
 403 the determined power trade schedule via the master problem is infeasible. Hence, inequality (78) as the
 404 feasibility cut should be created and provided back to the master problem.

$$\hat{F}_{t_b, h, t, s}^{IEH} + \Lambda_{t_b, h, t, s}^P \cdot (P_{h, t, s} - \hat{P}_{t_b, h, t, s}) \leq 0. \tag{78}$$

405 But if the optimal objective value $\hat{F}_{t_b, h, t, s}^{IEH}$ equals to zero, the determined power trade schedule will be

406 feasible. In this case, the optimal values of all slack variables will be equal to zero. Upon completion of the
 407 feasibility check phase, the IEHO will solve the optimality sub-problem in the second phase as presented
 408 in (79).

$$\begin{aligned}
 \text{Min : } & \hat{O}_{t_b, h}^{IEH}, \\
 \hat{O}_{t_b, h}^{IEH} = & \sum_{s \in \mathcal{S}} \sigma_s \cdot \left[\sum_{k \in \mathcal{K}} C_{k, s}^{CHP} + \sum_{e \in \mathcal{E}} C_{e, s}^{ES} + \sum_{q \in \mathcal{Q}} C_{q, s}^{P2H} + \sum_{\substack{(l, n) \in \\ (\mathcal{L}, \mathcal{N})}} C_{l, n, s}^{MDR} \right], \\
 \text{s.t. } & \text{Operational constraints of followers problems,} \\
 & P_{h, t, s} = \hat{P}_{t_b, h, t, s} \quad (\tau_{t_b, h, t, s}^P).
 \end{aligned} \tag{79}$$

409 where $\hat{O}_{t_b, h}^{IEH}$ signifies the minimized operation cost for the h th IEH under the determined power trade
 410 schedule, and $\tau_{t_b, h, t, s}^P$ is the dual variable associated with the second constraint of the problem (79).
 411 After that, an effective upper bound (UB) of the optimal two-stage robust-stochastic SCUC model can
 412 be calculated by (80).

$$UB = \hat{O}_{t_b}^{Total} + \sum_{h \in \mathcal{H}} (\hat{O}_{t_b, h}^{IEH} - O_h^{app}). \tag{80}$$

413 In each iteration, the convergence criterion of the Benders decomposition algorithm must be checked
 414 to decide whether it is necessary to perform the next iteration. A generally used convergence criterion is
 415 stated below:

$$|UB - LB| \leq \varepsilon. \tag{81}$$

416 where ε is a pre-defined value that indicates the convergence threshold. But if the convergence criterion
 417 is not met, the optimality cut should be constructed according to (82), and then added to the master
 418 problem. The flowchart of the proposed problem-solving process is shown in Fig. 4.

$$\hat{O}_{t_b, h}^{IEH} + \tau_{t_b, h, t, s}^P \cdot (P_{h, t, s} - \hat{P}_{t_b, h, t, s}) \leq O_h^{app}. \tag{82}$$

419 5. Case study and numerical results

420 In this section, the developed collaborative decision-making structure is applied to the modified IEEE
 421 30-bus test system to validate the feasibility and efficiency of the proposed decentral optimization program.
 422 The scheduling horizon is one day ($\mathcal{T} = 24$) with one-hour time slots. The numerical case studies are
 423 implemented in the environment of GAMS software on a personal computer with an Intel Core™ i7-4500
 424 CPU and 6-GB RAM. The proposed MILP problem is solved by commercial solver MOSEK in which the
 425 relative gap and the solution time limits are adjusted to 0.1% and 10000 s. Moreover, the convergence
 426 tolerance of the Benders decomposition algorithm is set at 0.05%.

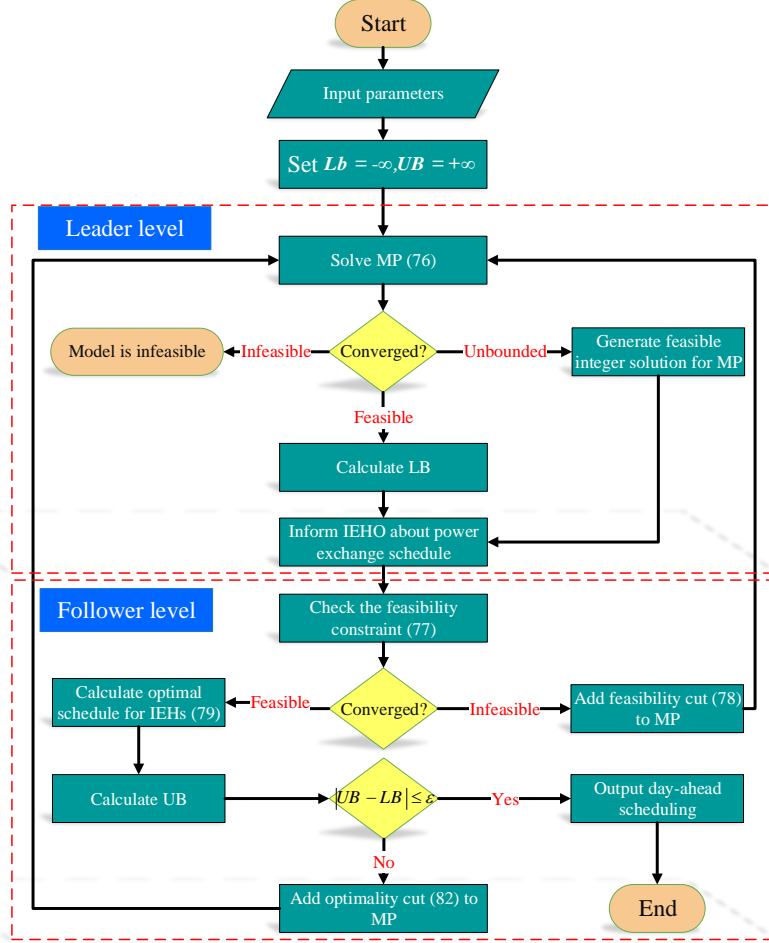


Fig. 4: Flowchart of the proposed algorithm.

5.1. Simulation setup

The topology of the modified test system is shown in Fig. 5. This test system is composed of two integrated areas. The first area is related to the renewable power system, which includes 30 buses, six conventional thermal units, 2 WFs, 2 PV parks, and 21 electrical loads. Bus 1 represents the slack bus, with a voltage phase angle of zero. All technical specifications associated with the 30-bus test system are provided in [38]. It should be noted that the capacity of transmission lines and technical parameters of thermal units were adjusted according to the peak load. The second area covers the two industrial parks that are equipped with IEHs. IEHs are committed to providing the electrical and heat demands of local industrial consumers located in industrial parks. Two IEHs are respectively located at buses 21 and 30, which are indicated by IEH1 and IEH2. Each IEH consists of a CHP unit, a EES system, and a P2H storage. Thus, in the whole integrated renewable energy system, there are two CHP units, two EES systems, and two P2H storages.

The predicted values related to each WF and PV park productions, as well as the hourly forecasted energy demands of all entities, are shown in Figs. 6 and 7. The rated capacity of WFs, PV parks installed on buses 12, 21, 23, and 30 are equal to 275, 325, 185, and 335 MW, respectively. It should be mentioned that candidate buses for the installation of RESs were selected in accordance with the results of the

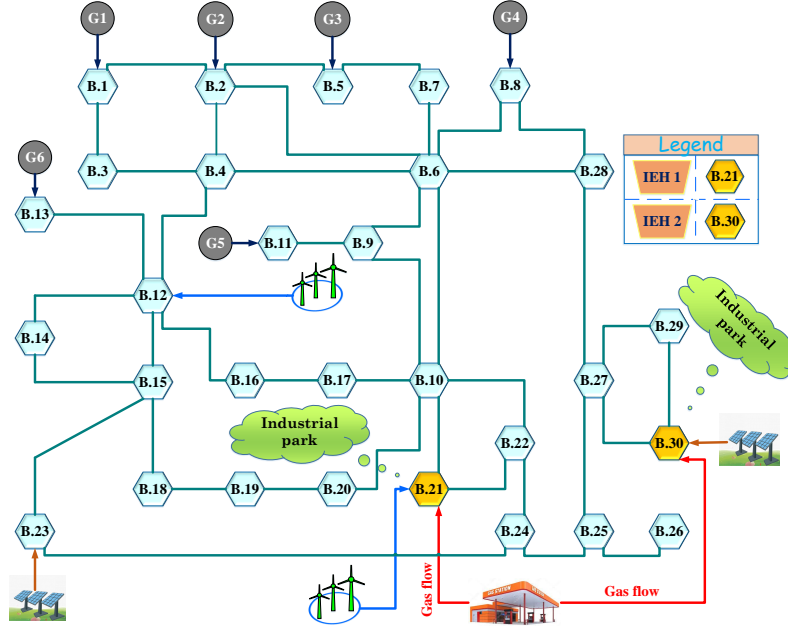


Fig. 5: Schematic of the proposed test system.

443 planning study carried out in [39]. In addition, all RESs produce active power at unity power factor.
 444 The share of each bus from the hourly electrical demand is presented in Fig. 8. Moreover, heat loads
 445 connected to the buses 21 and 30 have 40% and 60% share of the total heat demand, respectively. The
 446 characteristics of energy conversion facilities installed in IEHs are adopted from [40] and scaled to achieve
 447 180 MW of thermal energy. The essential technical characteristics are given in Table 2.

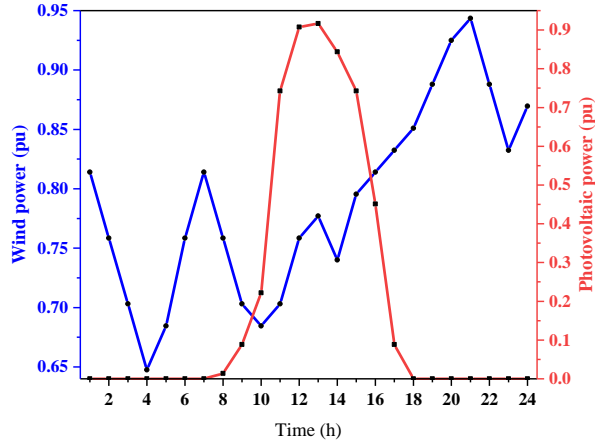


Fig. 6: Forecasted output power of each WF and PV park.

448 The penalty cost of renewable power curtailment (i.e., Π_{re}) is set to 120 \$/MW that is higher than
 449 the highest marginal cost of available thermal units, and the natural gas price (i.e., λ_g) is assumed to be
 450 15 \$/MWh [40]. The maintenance costs of CHP units (i.e., ρ_k) and P2H storages (i.e., ρ_q) are considered
 451 27 \$/MW and 50 \$/MW, respectively [41]. Also, the EES degradation cost (i.e., ρ_e) is 50 \$/MW [27].

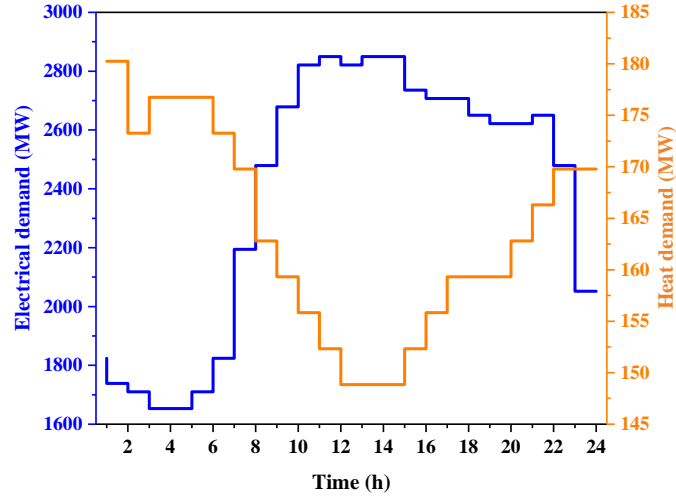


Fig. 7: Forecasted electricity and heat demands.

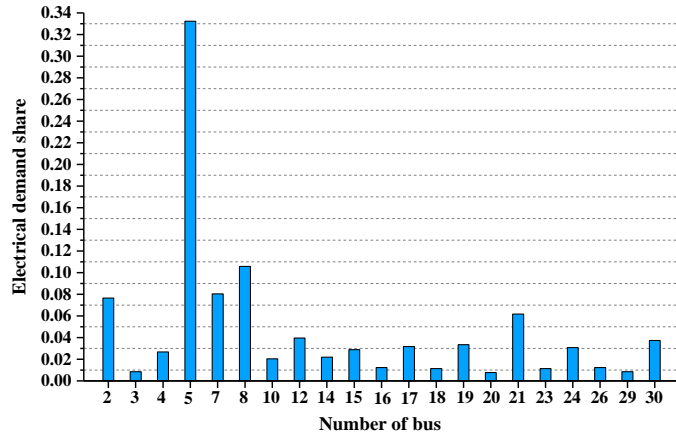


Fig. 8: Load share of each bus from hourly electrical demand of 30-bus test system..

Table 2: Specifications of the available equipment in IEHs.

Parameter	Amount	Parameter	Amount
η_k, η_q	0.35, 0.05	$\underline{A}_q, \overline{A}_q$ (MWh)	0, 60
$\eta_e^{ch}, \eta_e^{dch}$	0.9, 0.9	$\underline{P}_e^{ch}, \overline{P}_e^{ch}$ (MW)	5, 20
$\underline{P}_k, \overline{P}_k$ (MW)	45, 160	$\underline{P}_e^{dch}, \overline{P}_e^{dch}$ (MW)	5, 20
$\underline{H}_k, \overline{H}_k$ (MW)	0, 115	$\underline{A}_e, \overline{A}_e$ (MWh)	0, 60
\overline{P}_q (MW)	40	$\beta_{loss}, \beta_{gain}$	0.3, 0.6
$\overline{H}_q^{ch}, \overline{H}_q^{dis}$ (MW)	20, 20	COP_q	1.5

452 The incentive values for implementing multi-energy DRP are set to 20 \$/MWh and 10 \$/MWh for the
 453 electrical and heat loads, respectively. Furthermore, the coefficients α_l and α_n are assumed to be 15%
 454 and 10%, respectively.

455 Five case studies are considered to investigate the impact of the proposed structure on improving the
 456 performance of the integrated renewable energy system. These include:

- 457 • *Case 1*: The optimal collaborative operation of the high-renewable power system and IEHs is

analyzed in a decentralized manner. In this case, IEHs are equipped with only CHP units and various uncertain parameters are not considered;

- *Case 2*: The EES system is plugged into existing IEHs, and then the effects of electrical storage on case 1 are investigated;
- *Case 3*: Case 2 is developed with considering the role of P2H storage in achieving the desired goals;
- *Case 4*: The benefits of implementing multi-energy DRP on improving the techno-economic performance of the integrated renewable energy system are evaluated according to the IEHs formed in case 3. In this case, the uncertainties of renewable power production and energy demands are also ignored.
- *Case 5*: The proposed robust-stochastic SCUC model is applied to manage the uncertainties of the renewable power production and energy demands of the local industrial consumers with respect to privacy provisions. In this case, multi-energy DRP and all energy conversion facilities are considered.

The schematic of the proposed problem-solving process is shown in Fig. 9.

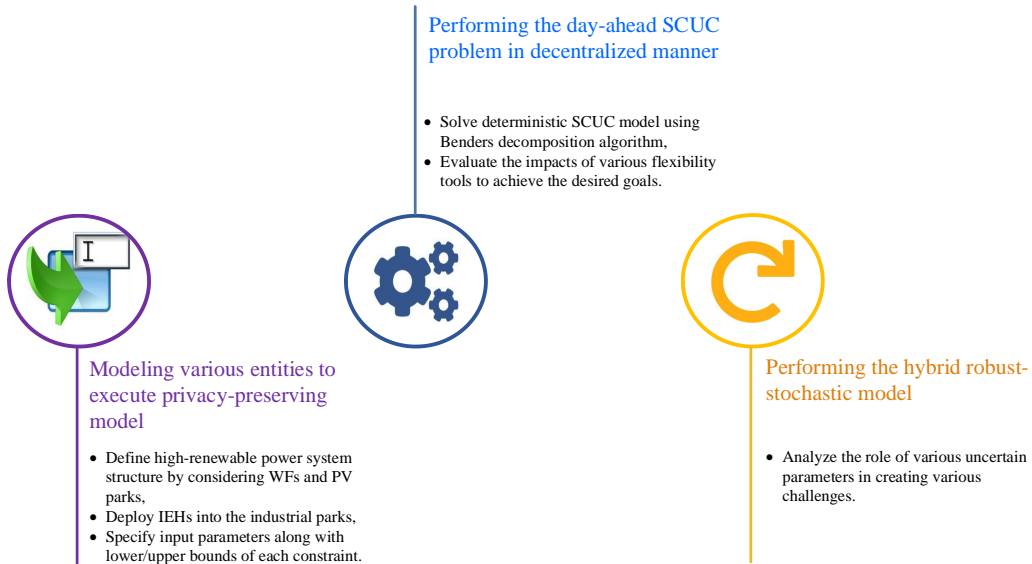


Fig. 9: The required steps to perform the simulation process.

5.2. Comparative results with/without various tools

To perform the collaborative operation scheme in terms of power trades, RPSO and IEHO optimize the scheduling of local energy resources by satisfying several operational/technical constraints in the renewable power system and IEHs. Figs. 10 and 11 show the total operation cost of the renewable power system and IEHs at each iteration of the Benders process for each case study. As can be seen, it takes 5, 5, 8, and 10 iterations to reach optimal results in cases 1 to 4, respectively. After proceeding the iterations, RPSO coordinates the scheduled power exchange with IEHO at each hour, according to the governing targets in each entity.

The hourly traded power between IEH1/IEH2 and the renewable power system for each case study are shown in Figs. 12 and 13, respectively. The negative values for traded power indicate that IEHs

481 are willing to deliver the surplus power to the renewable power system. As can be seen in these figures,
 482 regarding the capacity in each industrial park, IEH1 has more power demand from the renewable power
 483 system than IEH2 during the scheduling horizon. Meanwhile, IEH2 exhibits a higher tendency to transfer
 484 power to the renewable power system, specifically during the early and final intervals of the scheduling
 485 horizon. In both industrial areas, the highest traded power between IEHs and the renewable power system
 is related to case 3, where P2H storages are exploited as an efficient energy conversion facility.

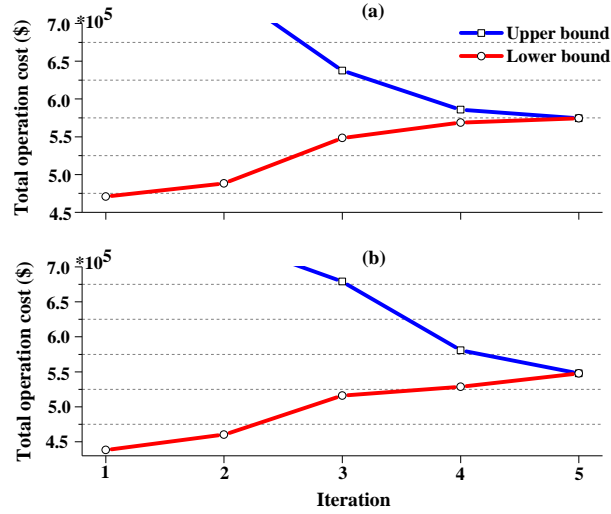


Fig. 10: Iteration process of Benders decomposition for (a) case 1 and (b) case 2.

486

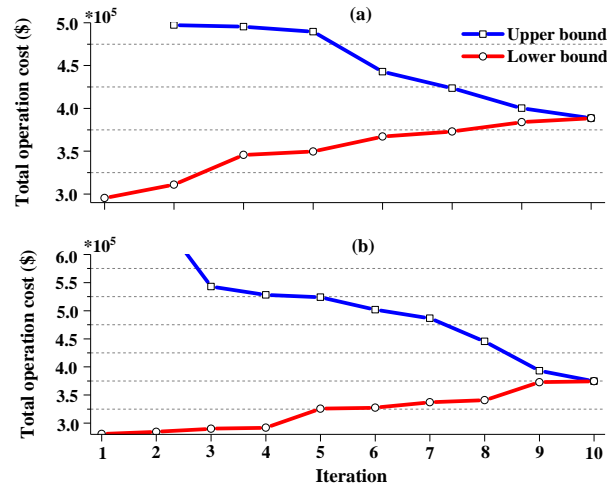


Fig. 11: Iteration process of Benders decomposition for (a) case 3 and (b) case 4.

487 Tables 3 and 4 present the total electrical and heat demands supplied by different resources for each
 488 case study. As it is evident from Table 3, the IEHs act as a viable option to increase the hosting capacity
 489 of RESs and reduce the participation of thermal units in meeting the electricity demand of the integrated
 490 renewable energy system. For instance, in cases 2, the power generated by thermal units during the
 491 scheduling horizon decreased by about 4,544 MW compared to the base case (without the deployment
 492 of IEHs). Therefore, the amount of spinning reserve provided by thermal units can increase by up to

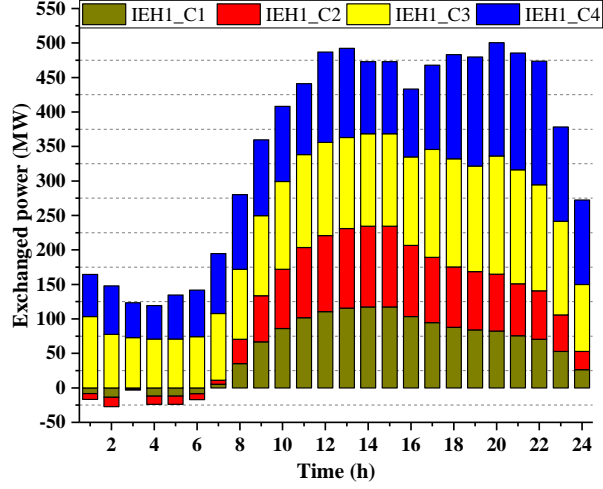


Fig. 12: Hourly traded power between IEH1 and renewable power system for each case study at bus 21.

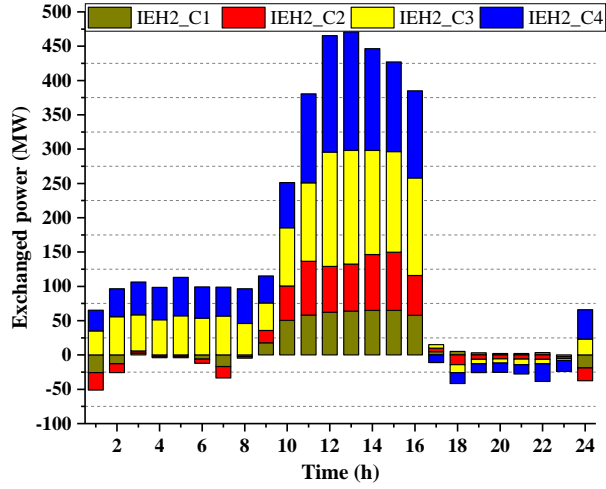


Fig. 13: Hourly traded power between IEH2 and renewable power system for each case study at bus 30.

493 10.2% by adopting the optimal coordinated strategy between the renewable power system and IEHs. In
 494 addition, case 4 demonstrates the capability of the proposed multi-energy DRP to enhance the reliability
 495 of the integrated renewable energy system by curtailing electrical demand (about 316 MW) using the
 496 DLC program. The distribution of the required demand among different sources, which are supported
 497 by different energy carriers, increases the flexibility and resilience of the renewable power system against
 498 potential risks associated with non-dispatchable power sources, natural disasters, and cyber attacks. From
 499 the heating point of view, CHP units act as the main supplier to cover the heat demand of industrial
 500 parks, which is due to its high production capacity.

501 The total amount of renewable power curtailment in each WF and PV park for each case study are also
 502 presented in Figs. 14 and 15. The results demonstrate that the proposed privacy-preserving structure is
 503 able to dramatically reduce renewable power curtailment with optimal collaborative expansion scheduling.
 504 In accordance with case 2, by adding EESs to IEHs under the title of backup power stations, it is found
 505 that the amount of curtailed renewable power reduces by 19.77% when compared to case 1. In case 3,

Table 3: Optimal mix of various sources to procure total electrical demand for each case study.

Total electrical demand (MW)	Case studies	Production of thermal units (MW)	Production of RESs (MW)	Production of CHP units (MW)	Production of EESs in discharging mode (MW)	Power delivered to EESs in charging mode (MW)	Power delivered to P2H storages (MW)	Load curtailment by multi-energy DRP (MW)
56,886	Base case	44,501.189	12,384.831	0	0	0	0	0
	Case 1	40,172.19	12,825.482	3,888.346	0	0	0	0
	Case 2	39,956.826	13,052.968	3,888.346	54.54	-66.66	0	0
	Case 3	41,646.616	13,904.825	2,184.067	81.978	-100.195	-831.27	0
	Case 4	41,212.74	13,959.254	2,074.721	18.635	-22.776	-673.512	316.956

Table 4: Optimal mix of various sources to procure total heat demand for each case study.

Total heat demand (MW)	Case studies	Production of CHP units (MW)	Production of P2H storages in direct mode (MW)	Production of P2H storages in discharging mode (MW)	Heat delivered to P2H storages in charging mode (MW)	Load curtailment by multi-energy DRP (MW)
3,938.609	Case 1	3,938.609	0	0	0	0
	Case 2	3,938.609	0	0	0	0
	Case 3	2,699.19	1,240.372	5.579	-6.533	0
	Case 4	2,822.277	1,010.269	0	0	106.063

506 the amount of curtailed renewable power significantly decreases in comparison with cases 1 and 2 by
507 incorporating the unique capabilities of P2H storages in the collaborative scheme to determine the power
508 trading schedule. In addition, with the simultaneous use of P2H storages and multi-energy DRP in the
509 collaborative scheduling approach among RPSO and IEHO, the values of curtailed wind and solar power
510 had reached zero and 16.5 MW, respectively. These simulation results clearly reveal that the promoted
511 IEHs in optimal coordination with the renewable power system had an effective role in reducing renewable
512 power curtailment.

513 In case 3, the effects of multi-energy DRP in coordination with EESs and P2H storages are evaluated
514 on the performance of IEHs to achieve the desired targets. It is assumed that the multi-energy DRP is
515 implemented only on the local industrial energy demands, which are located at buses 21 and 30. Figs. 16
516 and 17 show the consequence of implementing multi-energy DRP on the electrical and heat demands of the
517 industrial consumers connected to IEHs. According to these figures, the total electrical and heat demands
518 of the industrial consumers reduce by up to 5.62% and 2.7%, respectively, which is one of the reasons

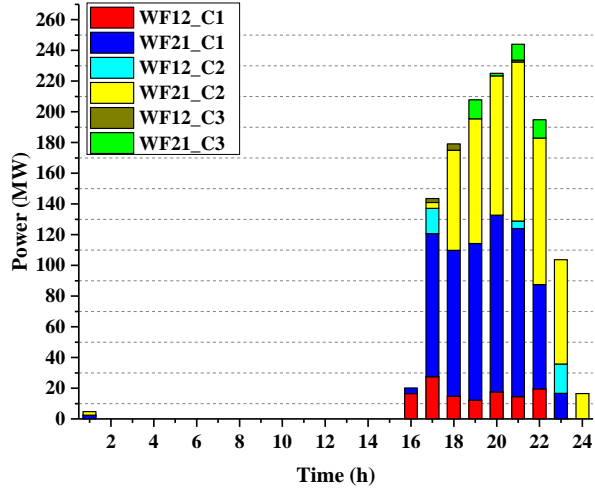


Fig. 14: Wind power curtailment for each case study.

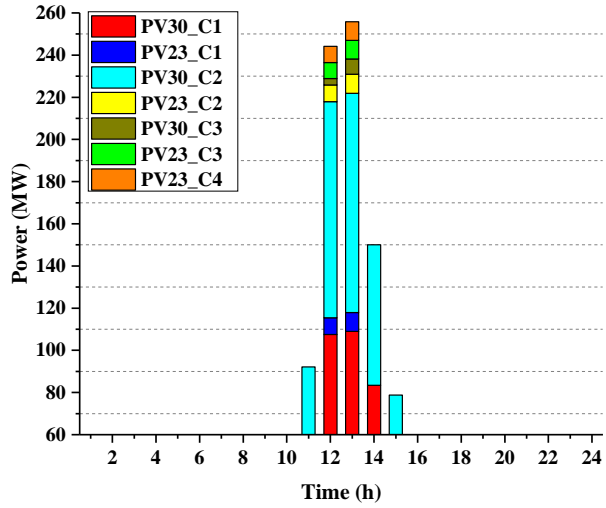


Fig. 15: Solar power curtailment for each case study.

519 for improving the performance of the integrated renewable energy system from the technical perspective.
520 To further analyze the impact of the multi-energy DRP on the operation cost, the sensitivities of the
521 renewable power curtailment cost and operation cost of IEHs to the multi-energy DRP participation rate
522 variations are analyzed. This analysis is very useful for IEHO and RPSO to harness existing opportunities
523 in the energy markets. The participation rates of electrical and heat demands for implementing multi-
524 energy DRP changed from $(\alpha_{l,n} - 8)\%$ to $(\alpha_{l,n} + 10)\%$ applying nine equal steps. The obtained results for
525 case 3 according to various participation rates are shown in Fig. 18. As can be seen from this figure, the
526 total operation cost of IEHs decreases almost linearly. On the other hand, there are almost no changes in
527 the renewable power curtailment cost up to values close to $(\alpha_l + 4)\%$ and $(\alpha_n + 4)\%$. But, the renewable
528 power curtailment cost dramatically increases with increasing the participation rates of electrical and heat
529 demands to more than $(\alpha_l + 4)\%$ and $(\alpha_n + 4)\%$. These results indicate that it is necessary to perform a
530 trade-off between different targets for the ideal utilization of the multi-energy DRP.

531 Table 5 presents a comprehensive economic comparison of different scheduling scenarios. As it is shown,

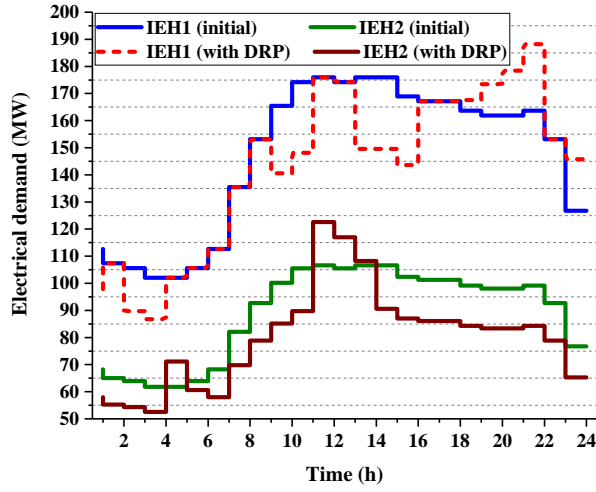


Fig. 16: The effect of multi-energy DRP on the local electrical demand of IEHs.

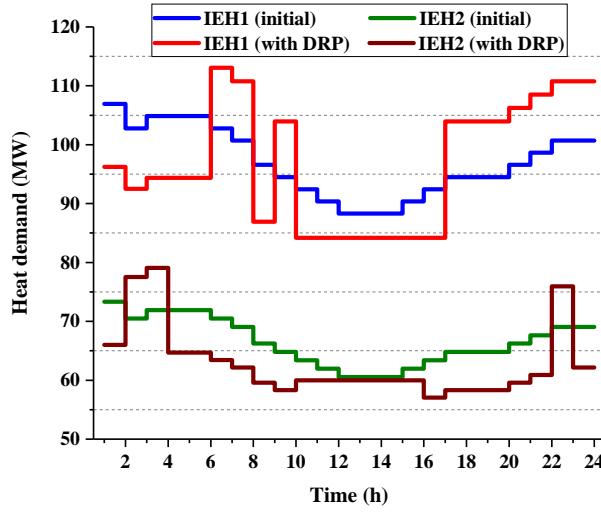


Fig. 17: The effect of multi-energy DRP on the local heat demand of IEHs.

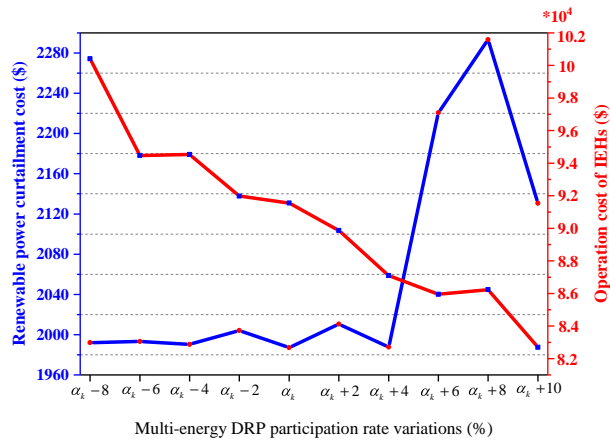


Fig. 18: Sensitivity of renewable power curtailment cost and operation cost of IEHs to the DRP participation rate.

532 the total operation cost of the renewable power system can be significantly reduced by deploying IEHs
533 in industrial parks according to a decentralized collaborative operation. In accordance with case 1, with
534 establishing IEHs along with the renewable power system under the title of sustainable energy producers,
535 it is found that the amount of total operation cost of renewable power system decreases by 21.4% when
536 compared to the base case. Moreover, the operation cost of the renewable power system decreases by up
537 to 27.72% in case 2, 44.99% in case 3, and 48.11% in case 4 compared to the base case by adding EESs
538 and P2H storage to each IEH as well as utilizing multi-energy DRP in the framework of IEHs. On the
539 other hand, the total operation cost of IEHs reduces from \$167,700 (case 1) to \$103,910 (case 3) by using
540 EESs and P2H storages. Finally, by examining the renewable power curtailment cost, which is reduced
541 from \$190,920 to \$1,987.07 by implementing the proposed privacy-preserving decision-making structure,
542 the impact of applying multi-energy DRP in the objective function is clearly revealed.

Table 5: Cost allocation for existing entities for each case study.

	Base case	Case 1	Case 2	Case 3	Case 4
Operation cost of thermal units (\$)	326,490	268,610	263,220	276,080	266,520
Cost of renewable power curtailment (\$)	190,920	138,040	110,740	8,518.49	1,987.07
Total operation cost of renewable power system (\$)	517410	406,650	373,960	284,598.49	268,507.07
Renewable power system operation cost decrement (%)	-	21.4	27.72	44.99	48.11
Operation cost of energy conversion facilities (\$)	0	167,700	173,760	103,910	91,556.62
Incentive compensation costs of multi-energy DRP (\$)	0	0	0	0	14,333.38
Total operation cost of IEHs (\$)	0	167,700	173,760	103,910	105,890

543 5.3. Impacts of uncertain parameters

544 To more clearly technical and economic analysis, the impacts of uncertain parameters, i.e., renewable
545 power production and electrical and heat demands of local industrial consumers, on the results of the
546 collaborative operation are investigated using the adjusted hybrid robust-stochastic model. The energy
547 demand prediction error follows a normal distribution function with a deviation of 10% and a mean of zero.
548 To this end, one-hundred scenarios are generated by MC simulation, which is reduced to ten scenarios by
549 the GAMS/SCENRED tool [42]. To handle the uncertainty associated with renewable power production,
550 the value of uncertainty budget, i.e., Γ_t , in the robust model is increased by steps 0.02 from 0.02 to 0.2. To
551 carry out the desired simulations, three different ranges for the maximum deviation between the forecasted
552 and actual values (i.e., $\tilde{P}_{x,t}$) are considered. The variation in the operation costs of the renewable power
553 system and IEHs for different Γ_t when $\tilde{P}_{x,t}$ changes from 10% to 30% are shown in Figs. 19 and 20. As can
554 be seen in Fig. 19, with increasing the amounts of Γ_t and $\tilde{P}_{x,t}$, the operation cost of the renewable power
555 system increases. The reason is that higher uncertainty budgets force RPSO to provide the required
556 power from expensive units instead of the RESs. Similarly, according to Fig. 20, with increasing the
557 robust approach parameters, the operation cost of IEHs also grows. However, although the operation cost

558 of IEHs has increased, the operation cost allocated to IEHs is still less than the deterministic method
 559 (\$105,890). This is due to the fact that by reducing the actual power generated by RESs compared to the
 560 forecasted value, the traded power between IEHs and the renewable power system also decreases. Traded
 561 power between IEH1/IEH2 and the renewable power system for $0.1P_{x,t}$ is shown in Fig. 21. As clearly
 562 visible, the total traded power between IEH1/IEH2 and renewable power system decreases from 4343.48
 563 MW, when $\Gamma_t = 0.02$, to 3665.33 MW, when $\Gamma_t = 0.2$, during the scheduling horizon.

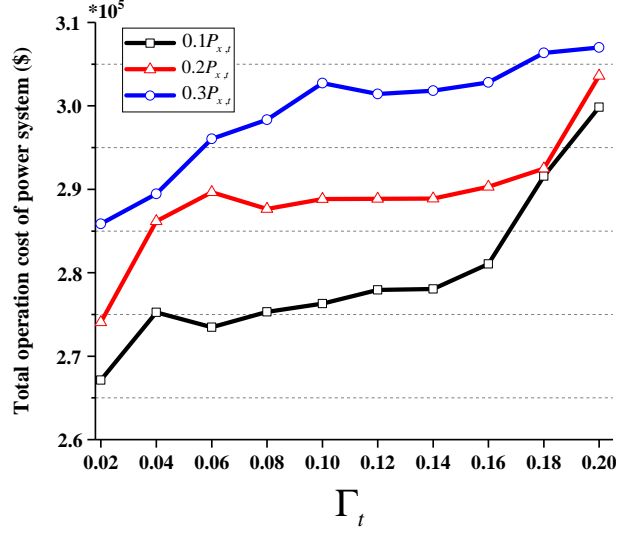


Fig. 19: Impact of Γ_t and $\tilde{P}_{x,t}$ on total operation cost of renewable power system.

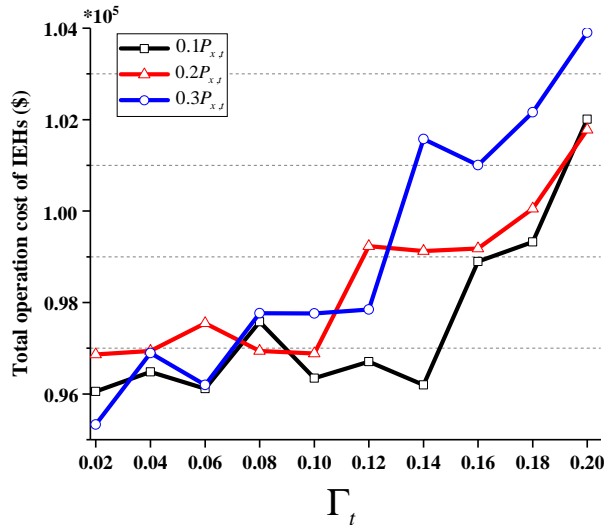


Fig. 20: Impact of Γ_t and $\tilde{P}_{x,t}$ on total operation cost of IEHs.

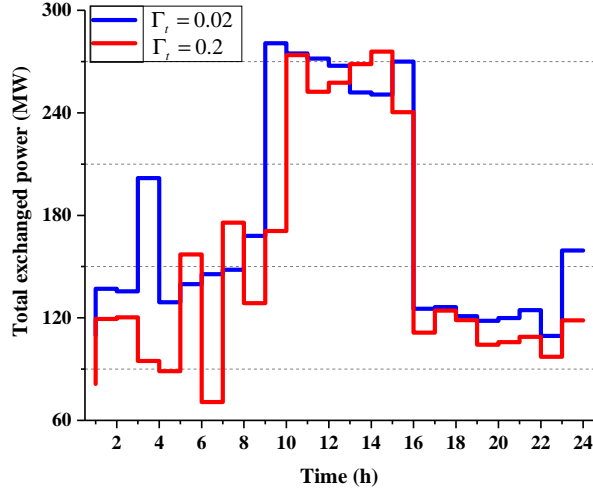


Fig. 21: The effect of variations of the uncertainty budgets on the total exchanged power.

6. Conclusions and future work

This paper presented a decentralized two-stage robust-stochastic model to achieve the optimal collaborative operation of private IEHs with the renewable power system in a privacy-preserving manner. In the presented collaboration structure, RPSO interacted with IEHs in the leader-follower fashion to perform the SCUC problem, while the Benders decomposition algorithm was exploited to resolve the conflicts of private entities. The main goal of the developed privacy-preserving decision-making structure was to minimize the operation costs of each private entity by relying on establishing a sustainable power trading schedule between IEHO and RPSO. The proposed model considered uncertainties in RESs power and energy demands of local industrial consumers, where CHP units, EESs, P2H storages, and multi-energy DRP served as flexible tools in the framework of IEHs. The obtained numerical results in the 30-bus test system confirmed the effectiveness of the proposed decentral solution in creating an economical and secure operation between IEHs and renewable power systems. The simulation results demonstrated that the total operating costs of the renewable power system and IEHs could reduce by up to 48.11% and 36.85%, respectively, using EESs, P2H storages, and multi-energy DRP. The results also showed the effect of P2H storage and multi-energy DRP on a significant reduction in renewable power curtailment.

In future work, we will focus on the transactive energy mechanism between multiple networked IEHs to enhance the flexibility and resiliency of the integrated renewable energy system.

Acknowledgment

Amjad Anvari-Moghaddam and Behnam Mohammadi acknowledge support of the “HeatReFlex-Green and Flexible Heating/Cooling” project (www.heatreflex.et.aau.dk) funded by Danida Fellowship Centre and the Ministry of Foreign Affairs of Denmark under the grant no. 18-M06-AAU.

References

- [1] D. Rakipour, H. Barati, Probabilistic optimization in operation of energy hub with participation of renewable energy resources and demand response, *Energy* 173 (2019) 384 – 399.
- [2] M. Zare Oskouei, A. Sadeghi Yazdankhah, Scenario-based stochastic optimal operation of wind, photovoltaic, pump-storage hybrid system in frequency- based pricing, *Energy Conversion and Management* 105 (2015) 1105 – 1114.
- [3] C.-H. Tsai, A. Figueroa-Acevedo, M. Boese, Y. Li, N. Mohan, J. Okullo, B. Heath, J. Bakke, Challenges of planning for high renewable futures: Experience in the u.s. midcontinent electricity market, *Renewable and Sustainable Energy Reviews* 131 (2020) 109992.
- [4] M. Z. Oskouei, B. Mohammadi-Ivatloo, M. Abapour, R. Razzaghi, Two-stage stochastic model for optimal scheduling of reconfigurable active distribution networks with renewable energy, in: 2019 9th International Conference on Power and Energy Systems (ICPES), 2019, pp. 1–5.
- [5] C. Viviescas, L. Lima, F. A. Diuana, E. Vasquez, C. Ludovique, G. N. Silva, V. Huback, L. Magalar, A. Szklo, A. F. Lucena, R. Schaeffer, J. R. Paredes, Contribution of variable renewable energy to increase energy security in latin america: Complementarity and climate change impacts on wind and solar resources, *Renewable and Sustainable Energy Reviews* 113 (2019) 109232.
- [6] Electric power annual 2014, u.s. energy information administration (EIA), [online]. available at: <http://www.eia.gov/electricity/annual/pdf/epa.pdf>.
- [7] M. R. Akhtari, M. Baneshi, Techno-economic assessment and optimization of a hybrid renewable co-supply of electricity, heat and hydrogen system to enhance performance by recovering excess electricity for a large energy consumer, *Energy Conversion and Management* 188 (2019) 131 – 141.
- [8] O. Abedinia, M. Zareinejad, M. H. Doranehgard, G. Fathi, N. Ghadimi, Optimal offering and bidding strategies of renewable energy based large consumer using a novel hybrid robust-stochastic approach, *Journal of Cleaner Production* 215 (2019) 878 – 889.
- [9] S. Yazdani, M. Deymi-Dashtebayaz, E. Salimipour, Comprehensive comparison on the ecological performance and environmental sustainability of three energy storage systems employed for a wind farm by using an emergy analysis, *Energy Conversion and Management* 191 (2019) 1 – 11.
- [10] X. Chen, C. Kang, M. O'Malley, Q. Xia, J. Bai, C. Liu, R. Sun, W. Wang, H. Li, Increasing the flexibility of combined heat and power for wind power integration in china: Modeling and implications, *IEEE Transactions on Power Systems* 30 (4) (2015) 1848–1857.
- [11] S. Rahmani, N. Amjady, Optimal operation strategy for multi-carrier energy systems including various energy converters by multi-objective information gap decision theory and enhanced directed search domain method, *Energy Conversion and Management* 198 (2019) 111804.

- 618 [12] T. Liu, D. Zhang, S. Wang, T. Wu, Standardized modelling and economic optimization of multi-
619 carrier energy systems considering energy storage and demand response, *Energy Conversion and*
620 *Management* 182 (2019) 126 – 142.
- 621 [13] Z. Jiang, Q. Ai, R. Hao, Integrated demand response mechanism for industrial energy system based
622 on multi-energy interaction, *IEEE Access* 7 (2019) 66336–66346.
- 623 [14] S. O. Sobhani, S. Sheykha, R. Madlener, An integrated two-level demand-side management game
624 applied to smart energy hubs with storage, *Energy* 206 (2020) 118017.
- 625 [15] C. Dang, J. Zhang, C. Kwong, L. Li, Demand side load management for big industrial energy users
626 under blockchain-based peer-to-peer electricity market, *IEEE Transactions on Smart Grid* 10 (6)
627 (2019) 6426–6435.
- 628 [16] M. J. Shabani, S. M. Moghaddas-Tafreshi, Fully-decentralized coordination for simultaneous hydro-
629 gen, power, and heat interaction in a multi-carrier-energy system considering private ownership,
630 *Electric Power Systems Research* 180 (2020) 106099.
- 631 [17] H. Gao, S. Xu, Y. Liu, L. Wang, Y. Xiang, J. Liu, Decentralized optimal operation model for coop-
632 erative microgrids considering renewable energy uncertainties, *Applied Energy* 262 (2020) 114579.
- 633 [18] A. Dini, S. Pirouzi, M. Norouzi, M. Lehtonen, Grid-connected energy hubs in the coordinated multi-
634 energy management based on day-ahead market framework, *Energy* 188 (2019) 116055.
- 635 [19] X. Lu, Z. Liu, L. Ma, L. Wang, K. Zhou, S. Yang, A robust optimization approach for coordinated
636 operation of multiple energy hubs, *Energy* 197 (2020) 117171.
- 637 [20] M. H. Shams, M. Shahabi, M. Kia, A. Heidari, M. Lotfi, M. Shafie-khah, J. P. Catalão, Optimal
638 operation of electrical and thermal resources in microgrids with energy hubs considering uncertainties,
639 *Energy* 187 (2019) 115949.
- 640 [21] A. A. Eladl, M. I. El-Affi, M. A. Saeed, M. M. El-Saadawi, Optimal operation of energy hubs inte-
641 grated with renewable energy sources and storage devices considering CO_2 emissions, *International*
642 *Journal of Electrical Power Energy Systems* 117 (2020) 105719.
- 643 [22] T. Liu, D. Zhang, T. Wu, Standardised modelling and optimisation of a system of interconnected
644 energy hubs considering multiple energies—electricity, gas, heating, and cooling, *Energy Conversion*
645 *and Management* 205 (2020) 112410.
- 646 [23] A. Bostan, M. S. Nazar, M. Shafie-khah, J. P. Catalão, Optimal scheduling of distribution systems
647 considering multiple downward energy hubs and demand response programs, *Energy* 190 (2020)
648 116349.
- 649 [24] X. Wang, Y. Liu, C. Liu, J. Liu, Coordinating energy management for multiple energy hubs: From a
650 transaction perspective, *International Journal of Electrical Power Energy Systems* 121 (2020) 106060.

- 651 [25] S. Bahrami, F. Aminifar, Exploiting the potential of energy hubs in power systems regulation services,
652 IEEE Transactions on Smart Grid 10 (5) (2019) 5600–5608.
- 653 [26] N. Nikmehr, Distributed robust operational optimization of networked microgrids embedded inter-
654 connected energy hubs, Energy 199 (2020) 117440.
- 655 [27] Y. Li, Z. Li, F. Wen, M. Shahidehpour, Privacy-preserving optimal dispatch for an integrated power
656 distribution and natural gas system in networked energy hubs, IEEE Transactions on Sustainable
657 Energy 10 (4) (2019) 2028–2038.
- 658 [28] Y. Zhou, M. Shahidehpour, Z. Wei, Z. Li, G. Sun, S. Chen, Distributionally robust co-optimization
659 of energy and reserve for combined distribution networks of power and district heating, IEEE Trans-
660 actions on Power Systems 35 (3) (2020) 2388–2398.
- 661 [29] Y. Zhou, M. Shahidehpour, Z. Wei, Z. Li, G. Sun, S. Chen, Distributionally robust unit commitment
662 in coordinated electricity and district heating networks, IEEE Transactions on Power Systems 35 (3)
663 (2020) 2155–2166.
- 664 [30] M. Carrion, J. M. Arroyo, A computationally efficient mixed-integer linear formulation for the thermal
665 unit commitment problem, IEEE Transactions on Power Systems 21 (3) (2006) 1371–1378.
- 666 [31] M. Yan, N. Zhang, X. Ai, M. Shahidehpour, C. Kang, J. Wen, Robust two-stage regional-district
667 scheduling of multi-carrier energy systems with a large penetration of wind power, IEEE Transactions
668 on Sustainable Energy 10 (3) (2019) 1227–1239.
- 669 [32] F. Teymoori Hamzehkolaei, N. Amjady, A techno-economic assessment for replacement of conven-
670 tional fossil fuel based technologies in animal farms with biogas fueled chp units, Renewable Energy
671 118 (2018) 602 – 614.
- 672 [33] M. Zare Oskouei, A. Sadeghi Yazdankhah, The role of coordinated load shifting and frequency-based
673 pricing strategies in maximizing hybrid system profit, Energy 135 (2017) 370 – 381.
- 674 [34] M. Alipour, K. Zare, B. Mohammadi-Ivatloo, Short-term scheduling of combined heat and power
675 generation units in the presence of demand response programs, Energy 71 (2014) 289 – 301.
- 676 [35] M. Mohiti, H. Monsef, H. Lesani, A decentralized robust model for coordinated operation of smart
677 distribution network and electric vehicle aggregators, International Journal of Electrical Power En-
678 ergy Systems 104 (2019) 853 – 867.
- 679 [36] D. Bertsimas, M. Sim, Robust discrete optimization and network flows, Mathematical Programming
680 98 (2003) 49 – 71.
- 681 [37] Z. Yuan, M. R. Hesamzadeh, Hierarchical coordination of tso-dso economic dispatch considering
682 large-scale integration of distributed energy resources, Applied Energy 195 (2017) 600 – 615.
- 683 [38] Gurobi optimization inc., "gurobi optimizer reference manual," 2014.

- 684 [39] K. Tian, W. Sun, D. Han, C. Yang, Coordinated planning with predetermined renewable energy
685 generation targets using extended two-stage robust optimization, *IEEE Access* 8 (2020) 2395–2407.
- 686 [40] M. A. Mirzaei, M. Z. Oskouei, B. Mohammadi-Ivatloo, , A. Loni, K. Zare, M. Marzband, M. Shafiee,
687 Integrated energy hub system based on power-to-gas and compressed air energy storage technologies
688 in the presence of multiple shiftable loads, *IET Generation, Transmission Distribution* 14 (2020)
689 2510–2519(9).
- 690 [41] M. Jadidbonab, B. Mohammadi-Ivatloo, M. Marzband, P. Siano, Short-term self-scheduling of virtual
691 energy hub plant within thermal energy market, *IEEE Transactions on Industrial Electronics* (2020)
692 1–1.
- 693 [42] Gams/scenred user guide, 2009. [online]. available at: <http://www.gams.com/>.